CT&F - Ciencia, Tecnología y Futuro
ISSN: 0122-5383
Instituto Colombiano del Petróleo (ICP) - ECOPETROL S.A.

Lopez Ramos, Eduardo; Gonzalez Penagos, Felipe; Rincón Martinez, Daniel Andrés; Moreno Gomez, Nestor Raul

DETACHMENT LEVELS OF COLOMBIAN CARIBBEAN MUD VOLCANOES

CT&F - Ciencia, Tecnología y Futuro, vol. 12, no. 2, 2022, July-December, pp. 49-77
Instituto Colombiano del Petróleo (ICP) - ECOPETROL S.A.

DOI: https://doi.org/10.29047/01225383.401

ARTICLE INFO
Received : November 25, 2021
Revised : June 28,2022
Accepted : April 10, 2023
CT&F - Ciencia, Tecnologia y Futuro Vol 12, Num 2 December 2022. pages 49 - 77
DOI: https://doi.org/10.29047/01225383.401

ctyf@ecopetrol.com.co

DETACHMENT LEVELS OF COLOMBIAN CARIBBEAN MUD VOLCANOES

NIVELES DE DESPEGUE DE VOLCANES DE LODOS DEL CARIBE COLOMBIANO

Eduardo Lopez Ramos[a], Felipe Gonzalez Penagos[b], Daniel Andrés Rincón Martinez[a], Nestor Raul Moreno Gomez[a].

ABSTRACT

Regional analysis of mud volcanoes shows the regional extension of these processes in Northern Colombia. Mud volcanoes are active systems with the characteristics of the underlying sedimentary sequences on the surface, as well as the presence of hydrocarbons. These provide information about the oil systems and the characterization of new migration paths. New data acquired during field geology studies, along with the evaluation of acquired aerial images by drones, allowed observation of variations in terms of morphology and neotectonic process, being distinctive among mud volcanoes formed on different structural domains. Mud volcanoes formed in basement areas without thrust faults (Hangingwall realm of the San Jacinto Fault) are usually circular, connected to the basement by regional faults. Other mud volcanoes formed in older and younger deformed belts (Footwall realm of the Sinú Fault and Footwall realm of the San Jacinto Fault respectively) tend to have ellipsoidal shapes, with drainage patterns that suggest local stress fields associated with regional strike-slip movements of major faults. The analysis of U/Pb ages in detrital zircons extracted from mud volcanoes and outcropping sedimentary sequences in the Colombian Caribbean, together with the analysis of foraminifera and palynomorphs, suggest different levels of detachment. Clay mineralogy and geochemistry indicate that mud volcanoes formed in the backstop and the Northern part of the San Jacinto deformed belt have sludge material from sedimentary sequences, with contribution from continental basement rocks, while the mud volcanoes in the central and Southern parts of the studied area tend to show sediments from deepest stratigraphic levels, derived from less evolved magmatic sources (dioritic basements). Gas and water analyses from studied mud volcanoes suggest that the old deformed belt, Paleocene accretionary wedge, and backstop areas, have evidence of thermogenic oil systems, while in the younger deformed belt domain, the tendency is to suggest microbial processes.

RESUMEN

El análisis regional de los volcanes de lodo muestra la extensión regional del fenómeno en el norte de Colombia. Los volcanes de lodo son sistemas activos que manifiestan las características de las secuencias sedimentarias subyacentes en la superficie, así como la presencia de hidrocarburos, lo que brinda información sobre los sistemas petroleros y la caracterización de nuevas rutas migratorias. Los nuevos datos adquiridos durante los trabajos de geología de campo, junto con la adquisición de imágenes aéreas por dron, permitieron observar variaciones en términos de morfología y procesos neotectónicos, siendo distintivos entre volcanes de lodo formados en diferentes dominios estructurales. Así, los volcanes de lodo formados en áreas de basamento no afectado por fallas inversas (Dominio del bloque colgante de la Falla de San Jacinto) suelen ser circulares, conectados al basamento por fallas regionales, mientras que los volcanes formados en cinturones deformados viejos y jóvenes (dominios de los bloques yacentes de las fallas de Sinú y San Jacinto respectivamente), tienden a presentar formas elipsoidales, con patrones de drenajes que sugieren campos de tensión local asociados a movimientos fallas rumbodeslizantes mayores. El análisis de edades U/Pb en circones detríticos extraidos de los volcanes de lodo y secuencias sedimentarias aflorantes en el Caribe Colombiano, sumado al análisis de faunas de foraminíferos y palinomorfos, sugieren niveles de despegue diversos. Los análisis de mineralogía y geoquímica de arcilla indican que los volcanes de lodo formados en el contrafuerte rígido y la parte norte del cinturón deformado de San Jacinto, tienen lodos originados en secuencias sedimentarias, con aportes de rocas de basamento continental, mientras que los volcanes de lodo ubicados en las partes central y sur de el área estudiada, tienden a mostrar lodos provistos desde niveles estratigráficos profundos derivados de fuentes ígneas menos evolucionadas (basamentos dioríticos). Los análisis de gas y agua obtenidos de varios volcanes de lodo sugieren que el antiguo cinturón deformado, la cuña de acreción del Paleoceno y las áreas de contrafuerte rígido, tienen evidencias de sistemas de petróleo termogénico, mientras que, en el dominio del cinturón deformado más joven, la tendencia es a mostrar evidencias de sistemas microbianos.

KEYWORDS / PALABRAS CLAVE

Mud volcanoes | Geochemistry | Northern Colombia | Petroleum systems
Volcanes de lodo | Norte de Colombia | Geoquímica | Sistemas petrolíferos

AFFILIATION

[a]*Empresa Colombia de Petróleos S.A, ECOPETROL.*
[b]*Ministerio de Minas y Energía.Calle 43 No. 57 - 31 CAN - Bogotá D.C., Colombia*
*email: Eduardo.lopezra@ecopetrol.com.co

1. INTRODUCTION

Mud volcanism or sedimentary volcanism is the result of the ejection or extrusion of mud, fluids and gases (Kassi *et al.*, 2014) controlled by the vertical migration of overpressured and liquefied fluids (Deville *et al.*, 2003; Martinelli and Judd, 2004; Ceramicola, *et al.*, 2020). It is common for the ejected products to form deposits that consolidate around the outlet orifice, which, based on the stacking of successive mudflows, give rise to conical or "volcano-shaped forms" (Hedberg, 1974; Deville *et al.*, 2006). Mud volcanoes are interpreted as the surface expression of subsurface mud diapir activity, which are subcompact units of mud or clay, out of equilibrium conditions of pressure and buoyancy with respect to their surroundings (Hedberg, 1974; Milkov, 2000; Kopf, 2002; Satyana and Asnidar, 2008; Mazzini and Etiope, 2017). Globally, sedimentary volcanism, specifically mud volcanism, is located in varied tectonic settings, covering marine and continental domains, with variable diameters and heights, as well as great diversity in the origin of transported fluids and solids. Global comparative studies show that mud extrusion occurs predominantly in collisional tectonic settings, initially as a result of fluid expulsion associated with porosity decrease by burial and later by hydrocarbon generation (Milkov, 2000; Kopf, 2002). As can be deduced from the definitions, the origin of mud volcanoes and mud diapirs are directly linked to the development of overpressure zones, which can be related to burial, tectonic, thermogenic-biogenic, and osmosis processes (Kopf, 2002; Kassi *et al.*, 2014), where burial and development of petroleum systems can occur in any tectonic or depositional setting. In recent decades, the study of large earthquakes on active margins suggests that mud volcanic eruptions are a direct consequence of compression during the phase of coseismic deformation (Jiang *et al.*, 2011; Baloglanov and Mamedova, 2018) or the formation of large period waves (Manga, et al., 2009; Bonini, et al., 2016).

In the Colombian Caribbean, there are numerous active mud volcanoes, which are commonly mentioned in works on shale tectonics, mud diapirism, and overpressured zone-forming processes (Hedberg, 1974; Reed *et al.*, 1990; Milkov, 2000; Kopf, 2002; Mazzini and Etiope, 2017). It has also been the subject of study in topics such as morphology (Correa *et al.*, 2007; Restrepo, et al., 2007; Carvajal and Mendivelso, 2017; Dill *et al.*, 2019; Rincón Martínez *et al.*, 2021; Rossello, et al., 2022), chemistry (Carvajal and Mendivelso, 2017; Dill and Kaufhold, 2018; di Luccio *et al.*, 2021), geophysics (Shepard, et al., 1968; Briceño and Vernette, 1992; Ghisays Ruiz *et al.*, 2020), biostratigraphy of ejected material (Trejos-Tamayo *et al.*, 2020) and natural hazards (Shepard, et al., 1968; Barrera, 2001). From these studies, it is noted that the origin and controlling mechanisms of mud volcanic activity in the Caribbean are varied, with some models emphasizing their relationship with faults (Reed *et al.*, 1990; Aristizábal, et al., 2009; Carvajal and Mendivelso, 2017), organic matter content in underlying sedimentary sequences (González-Morales *et al.*, 2015), or the influence of the saltwater wedge in coastal areas (Dill and Kaufhold, 2018). However, aspects of mud volcanism such as age, mud detachment levels, forming mechanisms, extension, evolution, and relationship with hydrocarbon manifestations remain poorly understood. Thus, this work presents a synthesis of field and laboratory investigations conducted in mud volcanoes in the Caribbean region of Colombia, focused on the area of the Lower Magdalena Valley and Sinú - San Jacinto sedimentary basins, and the compilation of geophysical data from the Sinú and Guajira offshore basins (Figure 1). The compendium of data obtained during this work on topics such as geomorphology, geochemistry, geophysics, provenance, and heavy minerals, allow us to propose scenarios of the possible rocks from which the mud diapirs detached, the fluids they contain, the possible mechanisms that formed the volcano or mud diapir, and its relationship with the tectonic or sedimentary environment in where it is located.

2. TECTONOSTRATIGRAPHIC FRAMEWORK

MORPHOLOGY OF THE CARIBBEAN COLOMBIA AREA

The Colombian Caribbean represents the transition from the South American continent to the Caribbean Sea. In the continental domain of the Colombian Caribbean, the Sierra Nevada de Santa Marta is one of the most outstanding morphostructural elements, with peaks higher than 4 km above sea level (a.s.l.), which is the southern boundary of the Guajira Offshore Basin and the eastern boundary of the Lower Magdalena Valley Basin. Another morphostructural element of regional extension is the Serranía del Sinú and Serranía de San Jacinto, which form the so-called Sinú - San Jacinto sedimentary basin, separating the Lower Magdalena Valley Basin from the Sinú Offshore Basin (ANH, 2005, 2007), with heights less than 2 km a.s.l. To the north, in the area of the La Guajira Peninsula, hills with elevations below 1 km a.s.l. form the Serranía de Macuira (Figure 1), as the continental boundary of the Guajira Offshore Basin (ANH, 2007). In the offshore domain, it is possible to identify the shelf zone, with variable amplitude from less than 1 km on the northern flank of the Sierra Nevada de Santa Marta, to more than 75 km in the Gulf of Morrosquillo (Figure 1).

Adjacent to the platform, the continental slope, also known as the Caribana slope (Tabares, et al., 1996), has a variable amplitude, ranging from less than 80 km to the northwest of the Sierra Nevada de Santa Marta, where most of the submarine canyons are concentrated, to more than 120 km in the Rancheria basin area, which is the zone with the lowest number of submarine canyons (Figure 1). The lower part of the Caribana slope is part of the Southern Caribbean Deformed Belt (Figure1), which is characterized by thrust belts with a northwestward tectonic advance direction (Kellogg and Bonini, 1982; Toto and Kellogg, 1992), except in the Magdalena Submarine Fan area, where high sedimentation rates seem to block regional structural advance (Breen, 1989). The abyssal plain zone in the Colombian Caribbean has been named Colombia Basin, where depths exceed 3,500 meters below sea level (m.b.s.l.), bounded to the south by the Southern Caribbean Deformed Belt and the Magdalena Submarine Fan, and to the northeast by the Aruba Gap (Figure 1).

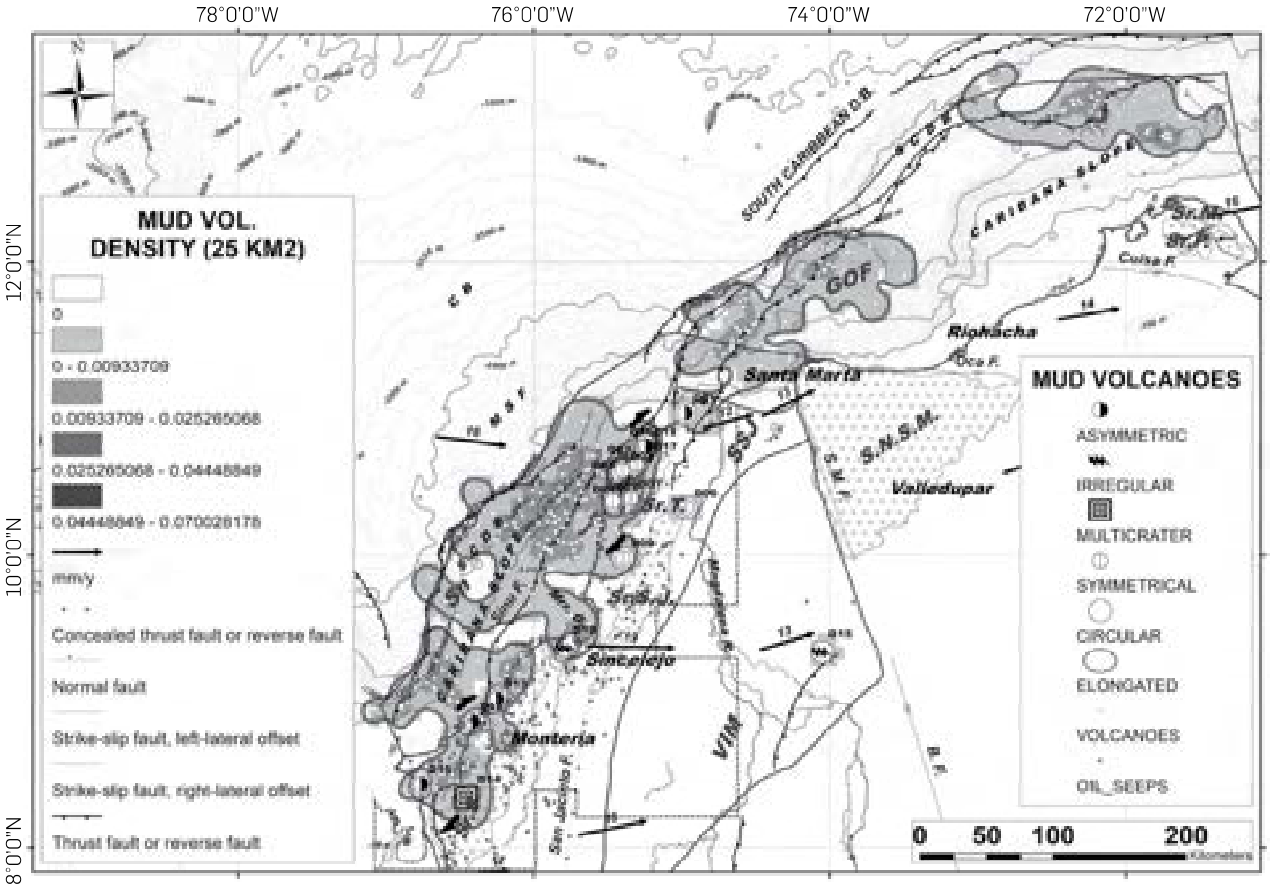

Figure 1. Figure 1. Location map of the study area and mud volcanoes analyzed (Letter D accompanied by numbers from 1 to 18 in dark bold show the location of the mud volcanoes studied, whose names are listed in Tables 2 and 3), with location of sedimentary basins (VIM: Lower Magdalena Basin; SSJ: Sinu - San Jacinto Basin; Sn.S.J.: Sinu - San Jacinto Basin; Sn: Sinu offshore basin; GOF: Guajira Offshore Basin; CB: Colombia Basin) taken from (ANH, 2007), geological mapping information (dark dotted line polygon), used in the location of mud volcanoes (Guzman and Hernandez, 1995; Guzman et al., 1998; Reyes, Barrera, et al., 1998; Barrera, 2001, 2003; Clavijo and Barrera, 2002; Geotec Ltda., 2003; Guzman, et al., 2003), trace of regional faults are modified from Gómez et al. (2015) and in the offshore of miscellaneous jobs (Toto and Kellogg, 1992; Kellog and Vega, 1995; Corredor, et al., 2003; Mantilla, 2007; Ceron-Abril, 2008; Quintero, 2012; Rincón Martínez et al., 2021). The names of the bathymetric features (Mrr. G.: Morrosquillo Gulf), and relevant morphostructural elements (SNSM: Sierra Nevada de Santa Marta; Sr.S: Serranía del Sinu; Sr.S.J.: Serranía de San Jacinto; Sr.T.: Serranía de Tubará; SCDB: Southern Caribbean Deformed Belt; Sr.M: Serranía de Macuira; Sr.P.: Seerranía de Parashi) are taken from Tabares et al. (1996). Note the distribution of mud volcanoes in the Colombian Caribbean (gray dots), and oil seeps (white dots), compiled from papers published in the onshore (Aristizábal et al., 2009; Carvajal and Mendivelso, 2017; Herrera Atencio & Díaz Mendoza, 2018) and offshore from review of seismic programs during this work and published papers (Shepard, et al., 1968; Briceño and Vernette, 1992; Quintero, 2012; H. Mora et al., 2018; Rincón Martínez et al., 2021), from which the density of diapirs per cell of 25km^2 was estimated in this work (Table 4), defining 4 blocks from south to north (thick gray lines). The ovals on the map are oriented according to the sigma 3 direction deduced from the morphological analysis on the analyzed mud volcanoes (Table 3), useful in the deduction of regional shear directions (in black), while the white circles show the mud volcanoes with circular shape. Symbols within ellipses and circles refer to topographic features of the volcanoes (from Table 1). Black arrows refer to the relative motion vectors of the Caribbean Plate with respect to the South American Plate (Mora-Páez et al., 2019).

GEOLOGY

Regionally, the Northern Colombian Caribbean zone comprises the northernmost part of the Central and Western tectonic domains, over which the Lower Magdalena Basin, Sinu San Jacinto Basin, Guajira Offshore Basin, and Sinu Basin are located (ANH, 2007). Regional geological and geochronological information from the Northwestern Corner of South America, suggests that western Colombia (from the Central Cordillera axis to the Pacific trench), has been the result of a continuous process of continental growth, by accretion of sequences related to oceanic affinity arc-crust, since the late Paleozoic (McCourt, et al., 1984). Accretion occurs along the South American continental margin, composed mainly by continental affinity rocks formed during Mesoproterozoic to Ordovician orogenic events (Cediel, et al., 2005; Restrepo-Pace and Cediel, 2010). This same continental growth process has been invoked for the formation of the Colombian Caribbean, from Early Cretaceous to Eocene, to explain the origin of the Serranía de San Jacinto (Kennan and Pindell, 2009; Cardona *et al.*, 2012; Flinch and Castillo, 2015), the northwestern portion of the Sierra Nevada de Santa Marta (Cardona *et al.*, 2010; Villagómez Díaz, 2010;

Bayona *et al.*, 2012; Zuluaga and Stowell, 2012) and western Guajira (Cardona *et al.*, 2009; Weber *et al.*, 2009). From the Oligocene to the Holocene, the Caribbean margin of Colombia in the Southern Caribbean Deformed Belt area and Serranía del Sinú, have grown mainly by structural stacking of accumulated sediments in the Colombia Basin and the advance of the Magdalena Submarine Fan (Duque-Caro, 1979; Toto and Kellogg, 1992; Corredor, et al., 2003; Cadena, et al., 2016).

The peripheral part of the Southern Caribbean Deformed Belt is predominantly composed of sediments accumulated during the Plio-Pleistocene, affected by thrust faults with NW tectonic advance direction (Corredor, et al., 2003; Rodríguez, 2020; López-Ramos *et al.*, 2021). Towards the interior of the Southern Caribbean Deformed Belt, a folded belt composed of thin Plio - Pleistocene and thick Miocene to Oligocene? sequences outcropping along the Serranía de San Jacinto and Serranía del Sinú belt is observed (Duque-Caro, 1979; Aguilera, 2011), with numerous offshore (Briceño and Vernette, 1992) and onshore (Carvajal and Mendivelso, 2017) active mud volcanoes. Published structural analyses suggest that the large number of active mud volcanoes along the Southern Caribbean Deformed Belt may be related to high fluid pressures in an area under compression (Toto and Kellogg, 1992), or by mud outflow through vertical conduits associated with wrench faults produced by accommodation of compressional structures (Aristizábal, et al., 2009) or extensional fractures formed on the crest of anticlines (Quintero, 2012).

CHRONOSTRATIGRAPHIC SETTING OF THE NORTHERN COLOMBIA BASINS

The Colombian Caribbean has a varied stratigraphic nomenclature, suggesting important chronostratigraphic and lithostratigraphic changes between basins such as the Lower Magdalena Valley, Sinú - San Jacinto, Sinú Offshore and Guajira Offshore (Table 1), delimiting "terrains" with their own stratigraphic characteristics such as the so-called Sinú Terrane, composed of sedimentary rocks accumulated predominantly during the Oligocene, while the San Jacinto Terrane is essentially composed of Paleocene rocks (Cediel, et al., 2005). Units such as the San Cayetano Fm. have been interpreted by some authors as a sequence bounded by regional unconformities, accumulated during the Paleocene (Aguilera, 2011; Laverde, 2000; Mora *et al.*, 2018), while other authors integrate the San Cayetano Fm. with formations such as Maco and Chengue (Cardona *et al.*, 2012; Flinch, 2003). A second sequence of regional expression, accumulated from the late Eocene to early Oligocene, composed of the San Jacinto and Tolú Viejo formations (Table 1), is characterized

Table 1. Correlation table of stratigraphic units for the Northern Caribbean of Colombia and the age of the sequences limited by regional unconformities defined in this work in the Colombian Caribbean. Ages, boundaries, and names of stratigraphic units were taken from published works (Aguilera, 2011; Bürgl, 1960; Cardona et al., 2012; Flinch, 2003; INGEOMINAS, 2009; Laverde, 2000; Mora et al., 2018; G. Rodríguez and Londoño, 2002).

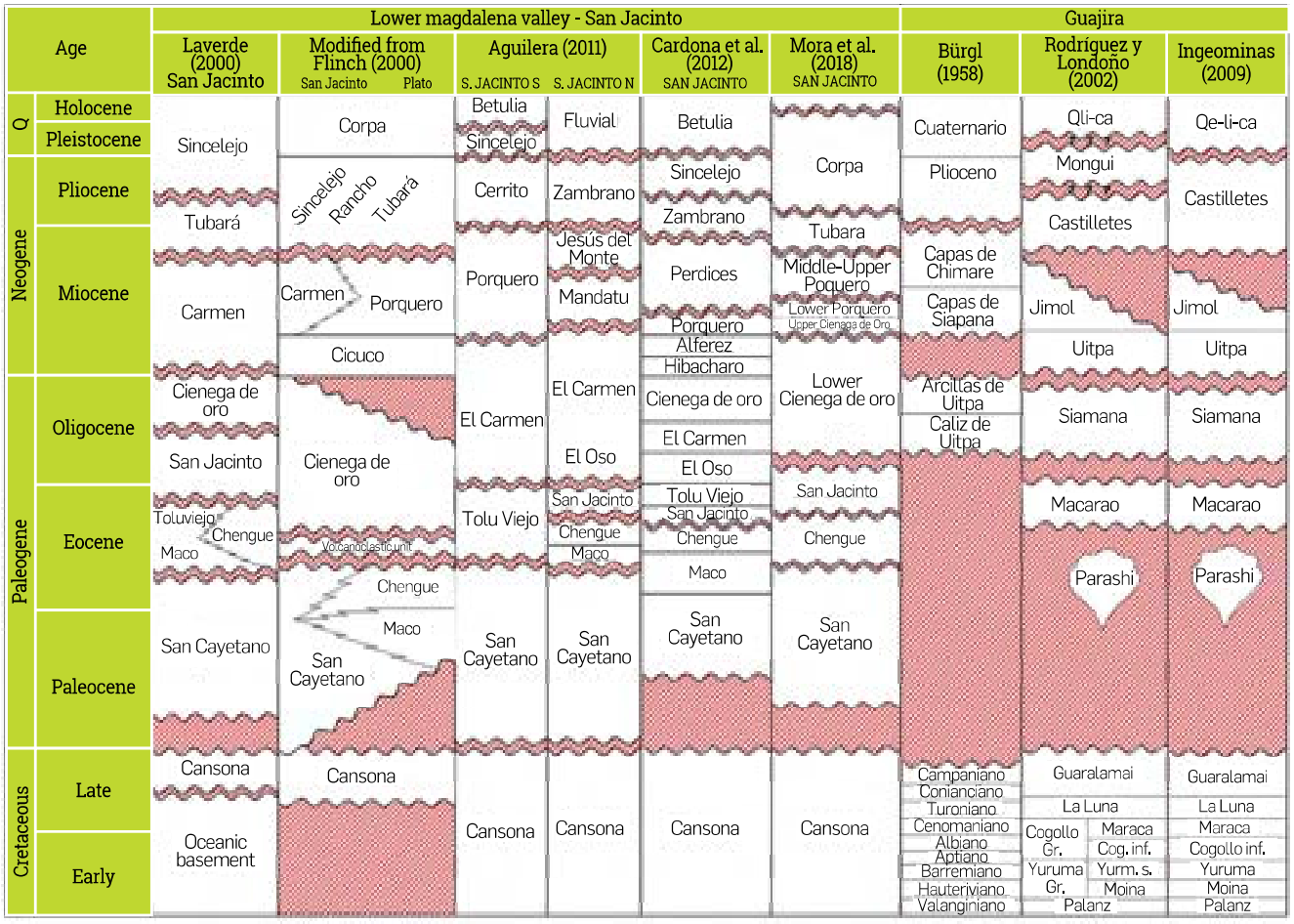

at the base by conglomeratic sandstones that grade upward to algal-rich limestone banks and nummulites (Cardona *et al.*, 2012; Mora *et al.*, 2018). A third sedimentary sequence, accumulated discordantly in the Lower Magdalena Basin and Sinú - San Jacinto Basin, from the early Oligocene to early Miocene, composed of formations such as Ciénaga de Oro, Carmen, Hibácharo, Alferes and Porquero (Table 1), is lithologically characterized by variable intercalations of mudstones and arenites (Aguilera, 2011; Geotec Ltda., 2003; Mora *et al.*, 2018, 2019). Several authors consider that most of the volcanoes and mud diapirs of the Colombian Caribbean are detached from this sequence, as well as the regional detachment level of the Southern Caribbean Deformed Belt thrusts (Aristizábal *et al.*, 2009; Duque-Caro, 1979; Flinch, 2003; Rodríguez, 2020). From the Middle Miocene to the Holocene, significant siliciclastic sedimentation of thicknesses greater than 4 km is registered in the Magdalena Submarine Fan area (Ceron-Abril, 2008; J. A. Martinez *et al.*, 2016; Basabe, 2018), as well as in the Guajira Offshore and Sinú offshore basins, while in the Lower Magdalena Valley and Sinú - San Jacinto basins they tend to decrease in thickness, as recorded by formations such as Sincelejo, Tubará, Corpa, Zambrano, Cerrito and Betulia -among others- (Table 1). The rocks of the latter sequence are intensely affected by mud volcano activity, intense deformation by mud diapirs and regional faults both onshore (Carvajal and Mendivelso, 2017) and offshore, where additionally numerous Mass Transport Complexes and Gravitational Gliding are observed (Leslie and Mann, 2016; Ortiz-Karpf, 2016; Naranjo-Vesga *et al.*, 2020).

In the area of La Guajira, cartographic and stratigraphic works (INGEOMINAS, 2009; Rodríguez and Londoño, 2002), show that in the northern part, there are Mesozoic sedimentary rocks of formations and groups such as Palanz, Yuruma, Cogollo, La Luna and Guaralamai, covered discordantly by sedimentary rocks of formations such as Macarao, Siamana, Uitpa - Jimol and Castilletes accumulated during the Cenozoic (Table 1). Igneous activity is reported during the Eocene, represented in the Parashi intrusive, synchronous to the final phase of intrusion and deformation of the Santa Marta batholith (Cardona, *et al.*, 2011; Villagómez *et al.*, 2011; Zuluaga and Stowell, 2012), a period in which a large temporal hiatus is evident (Table 1). In the northern part of the Guajira Offshore Basin, borehole-controlled seismic interpretations suggest the presence of sedimentary sequences of Cretaceous and Lower Paleocene - Eocene age, preserved in areas of continental basement affected by extensional fault systems (Martinez *et al.*, 2016). The greatest thicknesses of sedimentary sequences accumulated from the late Eocene to the Holocene in the Guajira Offshore Basin, are affected locally by transtensional fault systems (southern part of the Guajira Offshore Basin), gravity gliding and mud diapirism (Galindo, 2016; Martinez *et al.*, 2016).

3. DATA AND METHODOLOGY

DATA

The current study used more than 28,000 km of 2D reflection seismic lines, covering the entire Sinú offshore, Guajira Offshore, Sinú - San Jacinto and Lower Magdalena Valley basins, as well as the Magdalena Submarine Fan. This seismic information allowed to observe the subsurface expression of onshore and offshore mud volcanoes, and to locate active offshore mud volcanoes (Figure 1). We also integrated information from: a) digital elevation models with 30 m and 12 m resolutions (150,000 km^2), derived from global databases, used to identify mud volcanoes and associated structures; b) geologic mapping (45,000 km^2), scale 1:100,000 (Guzman and Hernandez, 1995; Guzman *et al.*, 1998; Reyes, Barbosa, *et al.*, 1998; Reyes, Barrera, *et al.*, 1998; Barrera, 2001, 2003; Clavijo and Barrera, 2002; Geotec Ltda., 2003; Guzman, et al., 2003), used to obtain the location of mud volcanoes and stratigraphic sequences affected by mud diapirism; c) more than 40,000 km2 of bathymetric information, used in the delimitation of offshore mud volcanoes. Additionally, radiometric dating information using the U/Pb technique in detrital zircons from outcropping sedimentary sequences was collected in the Sinú - San Jacinto Basin, as well as in Lower Magdalena Valley Basin, Sinú Offshore Basin and Guajira Offshore Basin wells (Cardona, V. A. Valencia, *et al.*, 2011; Cardona *et al.*, 2012; Lara *et al.*, 2013; Cardona and *et al.*, 2014; J Gómez *et al.*, 2015; Silva-Arias *et al.*, 2016).

The integration of all this information in a GIS environment enabled us to select 18 sites with active mud volcanoes (Figure 1), where the following activities were conducted: a) sampling of mud over active chimneys, for the extraction of detrital zircons, intended to obtain radiometric ages by isotopic techniques (U/Pb in zircons); b) identification of heavy minerals extracted from the mud expelled by the mud volcanoes; c) identification of clay minerals ejected by the mud volcanoes, using XRD techniques; d) petrography of clasts and blocks transported by the volcano to the surface; e) identification of foraminiferal faunas, calcareous nannofossils, and pollen transported to the surface by the mud; f) sampling of fluids and gases to determine the type and origin of the hydrocarbons in active mud volcano chimneys.

METHODOLOGY

The study began with a review of geological cartographic information, including the location of mud volcanoes in the continental domain of the Colombian Caribbean area (ANH, 2005). Furthermore, it relied on compiled publications and reports of mud volcanoes in the area (Guzman *et al.*, 1998; Reyes, *et al.*, 1998; Barrera, 2001, 2003; Geotec Ltda., 2003; Guzman, et al., 2003; Carvajal and Mendivelso, 2017), geophysical and tectonic studies (Shepard, et al., 1968; Aristizábal, et al., 2009; Domínguez *et al.*, 2010; Quintero, 2012; Bernal-Olaya, Mann and Vargas, 2016; Herrera Atencio and Díaz Mendoza, 2018; Ruiz *et al.*, 2020; Rincón Martínez *et al.*, 2021; Rossello, et al., 2022). Subsequently, volcanic cones were identified on the seafloor, with 2D and 3D seismic information, bathymetry and surveys developed to identify chimneys (Figure 1). The integration of these sources of information provided us with a regional distribution of mud volcanism in the onshore and offshore domains of the Colombian Caribbean area. With the processing of digital elevation models, parameters such as dome diameter (major and minor), and dome height, as well as elongations, drainage layout and hills around the main crater were calculated (Figure 2 and Table 2). This analysis allowed us to define easily accessible locations of recent volcanic mud activity (Figure 1), where mud and fluid samples were taken to: a) obtain the age of detrital zircons by U/Pb method to define the age of sources of sediments crossed by the mud diapir; b) extract fluids and gas from the active chimneys to analyse their geochemistry and postulate process of hydrocarbon formation; c) analyse the concentration of oxides and trace elements to identify the source of the sediments that make up the sedimentary sequences crossed by the mud diapirs; d) describe the micropaleontological content of mud and clast to identify the stratigraphic levels crossed by mud volcanoes; d) characterize the composition of the clast by petrography; e) extract heavy minerals. Mud samples were taken at the borders of the gryphons and craters

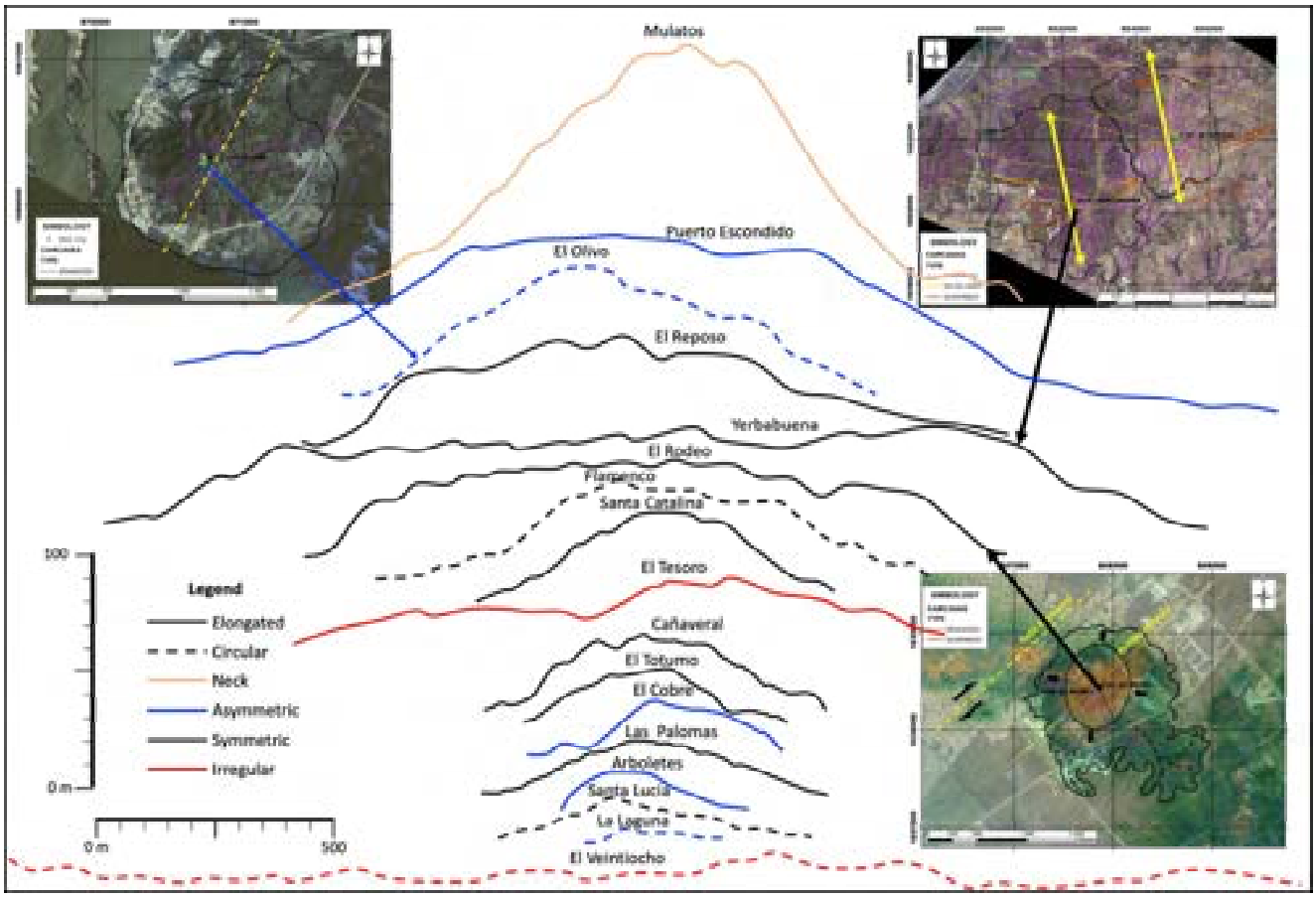

Figure 2. . Average topographic profiles of the volcanoes studied in the Colombian Caribbean (extracted from Digital Elevation Models with 12 m of resolution), with their degree of ellipticity and morphology (according to the geomophological descriptions summarized in table 2). The images show examples of some mud volcanoes with an elongate shape (right hand images), and asymmetrical circular shapes (upper left images).

of each of the mud volcanoes, using a 50 cm penetration, 1.5 cm diameter, stainless steel, hand-operated soil drill, extracting 150 g of sample per borehole. An average of 1,000 g of mud was taken for detrital zircons recovery, 1,000 g of sample for preservation, 250 g for biostratigraphic analysis, 250 g for chemical analysis of elements (major, minor and trace), 100 g for spectroradiometric calibration, and samples of mud-borne clasts for petrographic analysis. Fluid samples were collected in 5-liter containers, and gases were collected through a hood for final separation in the laboratory by decanting and filtering.

The mineralogical characterization of the clays was conducted by X-ray diffraction using a Rigaku Smartlab SE model equipment, which made it possible to: a) identify the clay minerals (phyllosilicates), and the non-clay minerals with an ordered internal structure; b) establish the mineralogical profile and the types of mineralogies present. Two modalities were used for this analysis: Total rock, or bulk and clay fraction. To correlate the characteristics of the clay minerals resulting from the burial processes to which the volcanics were subjected, measurements of the second reflections (002) in the spectra saturated with ethylene glycol were made to determine the proportion of Illite in the interstratified (I/Sm) and the direct relationship with the degree of ordering of each interstratified (R = Reichweite). Further, analyses of major, minor and trace oxide contents were performed on all samples.

Biostratigraphic analyses were performed in ICP laboratories (Instituto Colombiano del Petroleo). Samples for foraminiferal analysis were treated by the 10% hydrogen peroxide (H_2O_2) method due to the quality of the material (Sohn, 1961). Once the samples were prepared, they were sieved on 250 µm, 125 µm, 62.5 µm and 44 µm meshes. Subsequently, foraminifera were selected and assigned to a morphospecies to identify biozones along the sedimentary succession. Samples for calcareous nannofossil analysis were processed at the Geological Sample Processing Laboratory (LPMG) of the ICP, by the simple smear method (Bown and Young, 1998), which consists of cleaning the sample surface to avoid contamination, disintegrating a little sample on a slide, adding distilled water, and making a paste with a toothpick, rubbing it on the slide surface, and drying it on a drying plate. Subsequently, they were fixed on the surface with a coverslip, using diluted Canada balsam, with a previously labeled plate. The samples for palynological analysis were processed in the LPG laboratory of the ICP, following the protocol described in (Traverse, 2007) and the zonation was based mainly on the criteria proposed by (Jaramillo, Rueda and Torres, 2011), adjusting the ranges and stratigraphic positions of the key markers or taxa, based on the most recent analyses performed in the Colombian Caribbean offshore area.

Part of the mud volcano samples were processed to extract detrital zircons, in which U-Pb isotope analyses were performed, carried out

Table 2. Summary table of morphological characteristics of the 18 active mud volcanoes sampled. The numbers in the left column correspond to the numbers of the diapirs located on the map (Fig. 1). Columns of stage, shape, and type properties are described according to (Mazzini and Etiope, 2017). Topography is described according to topographic profiles (extracted and summarized in the Fig. 2). Geary and Moran shape profiles are described according to cross sections extracted from autocorrelation models in the selected mud volcano areas. Structural control and Sigma 3 columns describe the regional movements along faults, deduced from morphoestructural analysis.

Mud Volcano	Name	Stage	Shape	Roundness	Topography	Geary profile shape autocorre-lation	Moran profile shape autocorre-lation	Type	Structural Control	Sigma 3 Orientation
D01	La Laguna	Sleeping	Plateau-Low	Circular	Asymmetric	Cone	U	Bubblers		
D02	Las Palomas	Sleeping	Collapse	Elongated	Simmetric	plateau	U	Bubblers-Clast	Dextral shear	340
D03	Santa Catalina	Sleeping /Extinct	Sink-hole	Elongated	Simmetric	M	U	Splatters	Dextral shear	320
D04	Yerbabuena	Sleeping	Plateau-high	Elongated	Simmetric	MU	U	Bubblers	Dextral shear	350
D05	El reposo	Sleeping	Plateau-high	Elongated	Simmetric	I	U	Bubblers-Clast	Dextral shear	350
D06	Santa Lucia	Sleeping /Extinct	Conical	Circular	Simmetric	I	V	Clast rich		
D07	Cañaveral	Sleeping	Impact	Elongated	Simmetric	M	V	Splatters-Bubblers	Dextral shear	340
D08	El Rodeo Lateral	Sleeping	High plateau -multicrater	Elongated	Simmetric	MU	U	Splatters-Bubblers	Dextral shear	10
D08	El Rodeo Central	Sleeping	High plateau -multicrater	Elongated	Simmetric	MU	U	Splatters-Bubblers	Dextral shear	10
D09	Flamenco	Sleeping	Growing	Circular	Simmetric	M	U	Splatters-Bubblers		
D10	El Tesoro	Sleeping	Subsiding flanks	Elongated	Irregular	M	U	Bubblers	Dextral shear	330
D11	Virgen del cobre	Sleeping	Growing	Circular	Asimmetric	M	U	Bubblers		
D12	Arboletes	Sleeping	Plateau-Low	Elongated	Asimmetric	Cone	U	Bubblers		315
D13	Puerto escondido	Sleeping	Multicrater	Elongated	Asimmetric	MU	U	Splatters		330
D14	San Jose de Mulatos	Sleeping	Multicrater	Elongated	Stiff neck -multicrater	V	U	Bubblers-Clast		315
D15	El Veintiocho	Sleeping	Subsiding -multicrater	Circular	Irregular	I	R2	Splatters	Blocks	
D16	El Olivo	Sleeping	Growing	Elongated	Simmetric	M	V	Clast rich	Dextral shear	340
D17	El Totumo	Sleeping	Multicrater	Circular	Asimmetric	N	U	Splatters		
D18	Via al Totumo	Sleeping	Multicrater	Elongated	Asimmetric	N	U	Splatters		345

by Zirchron LLC laboratory (Tuczon, Az). Host rock samples were also analysed by this method to compare ages with those obtained from mud volcano samples. Samples for fission-track age analysis in zircons were subjected to mineral separation for heavy extraction using an electric pulse disgregator, selecting material between 25 and 500 microns in size, mounted on plates with epoxy and subsequently polished. Cathodoluminescence images were taken and U/Pb analyses were done with laser ablation ICP-MS, coupling a G2 193 nm excimer laser analyzer to the mass spectrometer. The U/Pb measurements were taken following the methodology proposed by (Chang *et al.*, 2006). For this work, the data and graphing of U/Pb results and calculation of ages were adapted to the methodology proposed by (Gehrels, 2012) selecting ages 206Pb/238U for <100Ma and 206Pb/207Pb for >1000 Ma, applying analytical uncertainty filters (not higher than 10%), analysis of concord, inverse discord and zircons of young ages (< 500 Ma). The data obtained were statistically analyzed and plotted according to the methodology from (Gehrels, 2012; Vermeesch, et al., 2016). Water, oil and gas (hydrocarbon and non-hydrocarbon) samples were extracted from the active volcanoes. The samples were treated in the field for preservation and shipment to the ICP laboratories, maintaining the cold chain. The results obtained were tabulated and taken to ArcGIS, where they were visualized in the form of bar diagrams, to observe the spatial variations of each method.

4. RESULTS

MORPHOLOGY

The integration of the results of the morphostructural analyses performed in the 18 mud volcanoes visited in the field during this project (Table 3), shows that more than 70% of the mud volcanoes have an elongated shape, with a direction of the major axis towards the NNE (Figure 1). Analysis of the lineaments and faults present in the area show that the elongated mud volcanoes exhibit some structural control, kinematically associated with dextral shear (Figures 1 and 2). Elongated-shaped volcanoes are concentrated in Serranía del Sinú (Figure 1), while circular shapes are concentrated in Serranía de San Jacinto and Lower Magdalena Basin (Figure 1). Morphostructural analysis shows that several of the elongate diapirs have kinematic signs of dextral shearing, with extensional vector direction ($\sigma 3$), with variable azimuth between 330º and 350°, linked to regional thrust fault movements with dextral component (Figures 1 and 2). Topographic profiles of diapiric domes show that they tend to be symmetrical in the area between Cartagena and Barranquilla, with some exceptions in volcanoes such as El Totumo and La Laguna, which are close to regional block boundaries (Figure

Table 3. Summary of ages obtained from palynological and micropaleontological analyses. The numbers in the left column correspond to the numbers of the diapirs (Table 1 and Fig. 1). Palino_young 1, bas 1, Top 2 and Bass 2 columns refers to age ranges of the two younger palynological associations, while Paly_oldest peak 1 and 2 refers columns refers to age ranges of the two oldest palynological associations obtained from samples recovered in mud volcanoes studied in this work. Column of Preservation Degree describe four categories of foram shells preservation: 1) Fair to bad; 2) Fair; 3) Fair to well; 4) Well preserved. The Foram recovery column describes the number of specimens recovered in each sample: 1) <15 specimens; 2) >15<40 specimens; 3) >40<100 speciments; 4) >100<400 specimens; 5) >400 specimens. Columns of younger and older Forams refers to the ages (younger and older) in Ma obtained from the micropaleontologial analysis of recovered specimens.

Mud Volcano	Name	Palino Young Top1	Palino Young Bas1	Palino Young Top2	Palino Young Bas2	Paly Oldest Peak1	Paly Oldest Peak2	Forams Recovery	Preservation Degree	Forams Younger	Forams Older
001	La Laguna	0	2			65		5	4	7	20
002	Las Palomas	0	56					2	2		
003	Santa Catalina	0	23					5	3	7	
004	Yerbabuena	0	7,2	23	48	70	65	4	3	7	14
005	El Reposo	0	55					4	2	7	
006	Santa Lucia	23	48					5	3	20	40
007	Cañaveral	5,3	23			70	65	2	2		
008	El Rodeo Lateral							4	1	5	20
008	El Rodeo Central							5	2	7	20
009	Flamenco	5	23					2	2		
010	El Tesoro	0	55					4	2	20	
011	Virgen del Cobre	7	12					4	3	4	20
012	Arboletes	7	12			70	65	4	4	5	20
013	Puerto Escondido	0	7					5	2	7	20
014	San Jose de Mulatos	0	55			65		4	2	7	
015	El Veintiocho	0	23					2	2		
016	El Olivo	5	23			34		2	2		
017	El Totumo	0	5			65		4	3	7	40
018	Via al Totumo	11,5	16,1			65		2	2		

2). To the south, in the Sinú area, diapiric domes tend to present asymmetric topographic profiles (Figure 2), especially those located near regional block-limiting faults. The status of the volcanoes (Mazzini and Etiope, 2017) is predominantly dormant, with one in an inactive state - Santa Lucía - and the rest of them being inactive (Yerbabuena, Arboletes and El Totumo).

XRD CLAY CHARACTERIZATION

The mineralogical characterization by X-Ray Diffraction (XRD) of the sediment samples of mud volcanoes taken in the Colombian Caribbean onshore area shows similar mineralogies at mass level, predominantly quartz-rich clay minerals (phyllosilicates), with values between 56% and 78%, enriched in quartz, with values between 22% and 35%, except for sediments of El Rodeo, El Tesoro, and Virgen del Cobre mud volcanoes, with quartz content below 20%. In smaller proportion, sodium feldspar and/or plagioclase are observed, which do not exceed 8%, potassium feldspar with maximum values of 6%. Calcite type carbonates not exceeding 5%, and Pyrite at trace level. Among the clay minerals, characterized at the level of the fraction smaller than 2 µm, Chlorite predominates, especially in the volcanics studied in Serranía del Sinú, while Smectite predominates mainly in the volcanics studied in the northern part between Barranquilla and Cartagena, in Serranía de San Jacinto, Serranía de Tubará, and Lower Magdalena Basin (Figure 3). Another clay mineral detected is Illite, which in subsequent treatments shows low crystallinity indices in the southern and central part of Serranía del Sinú, increasing its degree of crystallinity towards the north of it. The crystallinity of kaolinite varies from 0.3 to 0.4 Δ °2θ, especially in the southern part of the Sinú - San Jacinto basin, decreasing to 0.15 Δ °2θ along the Serranía de Tubará and Lower Magdalena Basin in mud volcanoes such as El Totumo, El Veintiocho, Santa Catalina, and La Laguna (Figure 3).

The saturation of clays with ethylene glycol shows two clear diagenetic trends, one with very shallow burial levels and Illite percentages between 10-40% within the interstratified I/Sm, and the other with much higher levels, between 60-75% associated with more advanced diagenetic states and correlatable with higher burial conditions and temperature. Preliminary analyses suggest the presence of several smectite phases in most of the samples, with smectite contents ranging between 2 and 8%, a value that was quantified in the Bulk fraction. To expand the analysis of some of these samples, they were treated with Li. The samples corresponding to the mud volcanoes La Laguna, Santa Catalina, El Reposo, Yerbabuena, El Rodeo, and Flamenco, show the presence of two smectite phases: one of Montmorillonite type, signal remaining at 10Å, and another possibly of the Beidelite type, band between 14-17Å. On the contrary, the behaviour of the samples in mud volcanoes such as Las Palomas, Santa Lucía, Cañaveral, Flamenco, Rodeo Lateral, Virgen del Cobre, Arboletes, and Puerto Escondido during treatment with Li at 300 ºC and Li at 300 ºC with glycerol, evidence of the closure and permanence of a single signal at 10Å, thus confirming the presence of Montmorillonite.

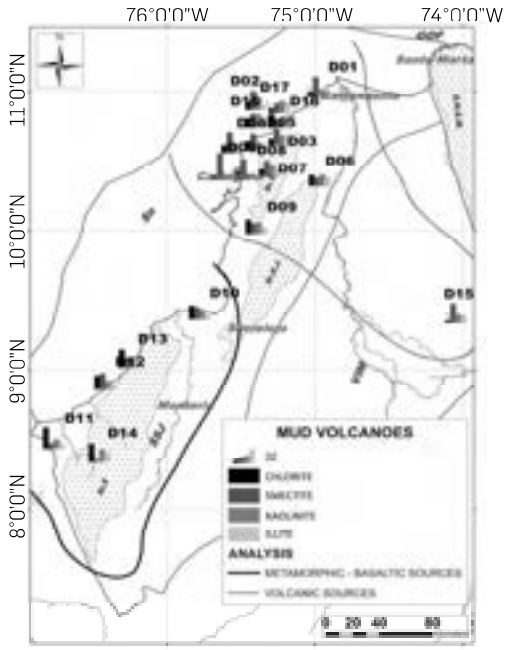

Figure 3. Location map of mud volcano samples analyzed by XRD. The bars indicate the percentages of the main clay minerals obtained in each mud volcano and the numerical values correspond to the corrected crystallinity indexes of illite. Note that the highest contents of smectite are concentrated in the northern part of the Serranía de San Jacinto (Sr.S.J.) and Serranía de Tubará (Sr.T.), while to the south, along the Serranía del Sinú (Sr. S) and southern part of the Sinú - San Jacinto Basin (SSJ), mud volcanoes tend to have higher contents of chlorite.

INORGANIC GEOCHEMISTRY

Geochemical analyses were conducted on mud volcano samples, obtaining 10 major and 38 minor and trace elements. The results show variability in the content of the different oxides, with SiO_2 and Al_2O_3 being the most variable and with the highest relative contents. The mobility and immobility of elements in the sedimentary medium were evaluated by the construction of pairs of element scatter plots, especially with respect to Al_2O_3, which is a relatively immobile element. Some works (Amajor, 1987) used the TiO_2 vs Al_2O_3 and La/Sc versus Th/Co binary plots to distinguish between granitic and basaltic source rocks. Applying the TiO_2 vs Al_2O_3 plot (Figure 4) revealed that the studied shale extracted from mud volcanoes define two main families: a) Family 1, characterized by a positive linear correlation, especially from samples extracted from mud volcanoes located in the Lower Magdalena Basin, northern part of Serranía de San Jacinto and Serranía de Tubará (Figure 4); b) Family 2, characterized by major TiO_2 concentrations, describing a trend above the positive linear correlation observed in Family 1, especially in samples from mud volcanoes along Serranía del Sinú (Figure 4). The scatter plot of La/Sc versus Th/Co shows that the Family 1 of mud volcanoes tend to have ratios of these elements above 0.7 and 0.5 respectively, while Family 2 of mud volcanoes tend to have lower ratios (Figure 4). The scatter plot of Al_2O_3/P_2O_5 vs Th/La (Figure 5) is useful to define the proportion of terrigenous, hydrogenous and volcaniclastic sources in marine sediments (Planke, 2005). The analysed samples of shales showTh/La values between 0.3 and 0.4 for the mud volcanoes located along Serranía del Sinú, Serranía de San Jacinto, and to the west of the Serranía de Tubará, while Th/La values above 0.4 are concentrated in Serranía de Tubará and Lower

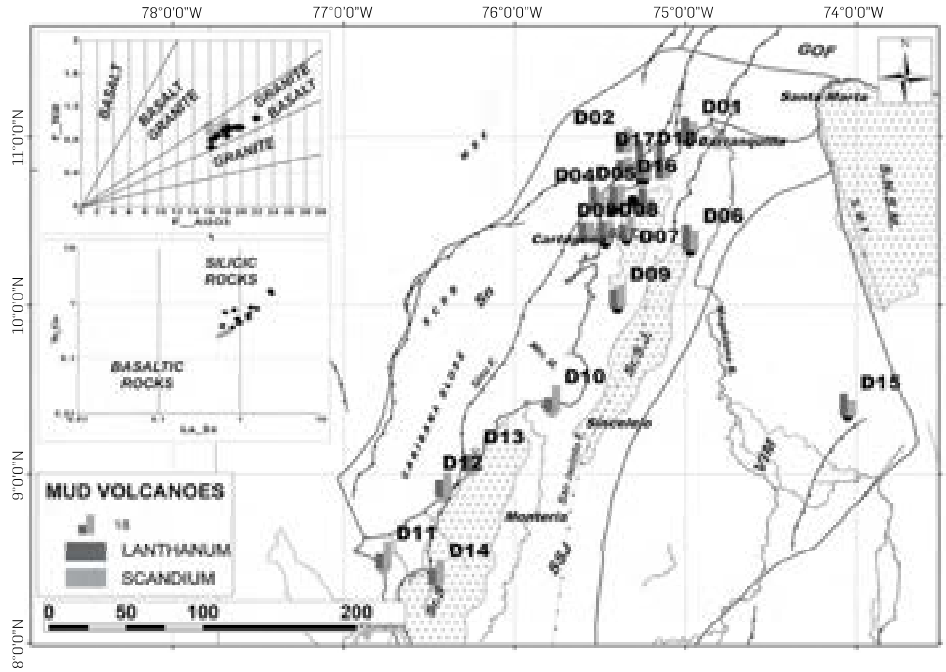

Figure 4. Location map of mud volcano samples with analysis of major oxides (gray and black dots) and trace elements (Lanthanum-Scandium percentages in bar diagrams). On the left, provenance diagrams of Al_2O_3 vs TiO_2 and Th/Co vs La/Sc (Amajor, 1987; El-Wekeil and El-Anwar, 2013; Chen et al., 2016; Mitra, Chakrabarti and Shome, 2018), the black dots refer to the samples from the volcanoes studied at Serranía del Sinú (Sr. S.J.), Lower Magdalena Basin (VIM) and Serranía de Tubará (Sr. T.), while the gray dots refer to the mud volcanoes studied at Serranía del Sinú (Sr. S). Note the tendency to present genetic relationships with granitic-silicic rocks in the northern mud volcanoes, while to the south, they tend to basaltic sources. The bar diagrams show the Lanthanum and Scandium content in sampled mud volcanoes, with Lanthanum predominating in the northern volcanoes and Scandium to the south.

Magdalena Basin (Figure 5). In contrast, the Al_2O_3/P_2O_5 values show a wide range, from 35 to 160, with no particular spatial relation to the distribution of the mud volcanoes analyzed (Figure 5).

U/Pb AGE POPULATIONS IN DETRITAL ZIRCONS EXTRACTED FROM MUD VOLCANOES

The processing of sediments extracted from the active gryphons of the mud volcanoes analyzed in the Colombian Caribbean during this work allowed the recovery of sufficient quantities of detrital zircon crystals for U/Pb dating. These detrital zircons have been transported to the surface by dragging during the intrusion of overpressured mud through the sedimentary sequences. In general, zircon recoveries were abundant, between 80 and 250 zircons, selecting for each sample 206Pb/238Pb ages for <1,000 My and 206Pb/207Pb ages for >1,000 My. Analytical uncertainty filters (less than 10%), concordance analysis, inverse discordance and young zircon ages <500 My were applied to the data. All data were statistically analyzed and represented in Probability vs. Age plots for ages <500 My, as well as Density plotter and DZage to define the first representative statistical population of ages. Based on this analysis, we were able to discriminate an average of teen U/Pb age populations for each mud sample, with crystal structure closure ages from 1 to 1,500 My, and to extract the youngest zircon grain age (values between 1 and 67 My). The age populations obtained were compared with detrital zircons ages reported in Meso-Cenozoic sequences outcropping in the Sinú and San Jacinto mountain ranges to establish possible stratigraphic levels of detachment of the mud rising through the mud volcanoes.

The age of the youngest zircon grain extracted shows that values above 24 My tend to be found in mud extracted from mud volcanoes in the northern part of Serranía de San Jacinto and Serranía de Tubará, while values below 24 My are characteristic of muds recovered from near-shore mud volcanoes, especially along Serranía del Sinú and northern Serranía de Tubará (Figure 6). The youngest U/Pb population age (first relative age frequency peak) obtained from the analyzed mud samples shows a geographic distribution similar to that observed for the youngest zircon grains. Thus, relative frequency values above 69 My are observed along Serranía de Tubará and Serranía de San Jacinto, north of VIM and punctually south of Serranía del Sinú, in the San José de Mulatos mud volcano (Figure 7), and lower than 69 My in the northern part of Serranía del Sinú and Serranía de Tubará (Figure 6). This geographic distribution holds when selecting the four youngest populations of U/Pb ages (first four peaks of relative age frequency), tending to be lower than 69 My in the mud volcanics along the Serranía del Sinú and Serranía de San Jacinto, while towards Serranía de Tubará, values tend to be greater than 69 My (Figure 8). A similar distribution pattern is maintained when extracting the four oldest populations (last 4 relative age frequency peaks), tending to present zircons with Neoproterozoic and lower Palaeozoic ages in the Serranía de Tubará and northern Serranía de San Jacinto zone, while in the southern Serranía de San Jacinto and Serranía del Sinú zone, there is a tendency to recover zircons of Mesozoic - Cenozoic ages (Figure 8).

COINCIDENT CLUSTERING OF U/Pb AGE POPULATIONS IN DETRITAL ZIRCONS BETWEEN MUD VOLCANOES AND SEDIMENTARY FORMATIONS

Considering that the zircons recovered from mud volcanoes result from the concentration of minerals during their ascension to the surface, a comparative exercise of ages of detrital zircons from the probable source or host rock, with those obtained in the zircons extracted from mud volcanoes was performed. For this exercise, we used U/Pb age values in detrital zircons from ninety samples obtained from outcropping sedimentary formations in previous works, along the Serranía de San Jacinto, Serranía de Tubará and Serranía del Sinú (Figure 9), compiled from published works (Cardona *et al.*, 2009, 2012; Villagómez Díaz, 2010; Cardona. *et*

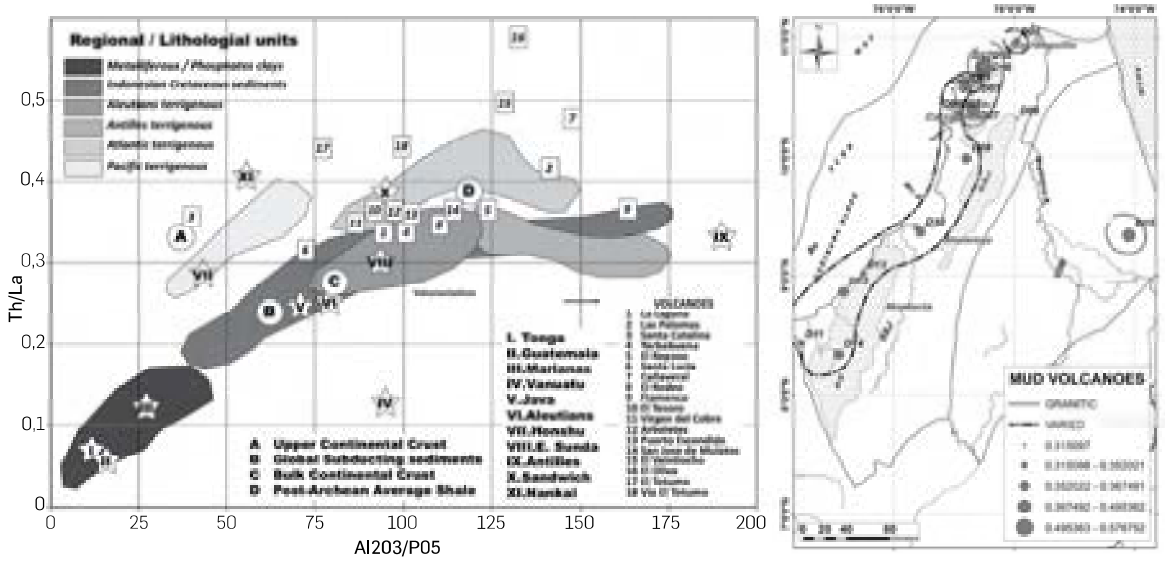

Figure 5. Left Correlation plot of Th/La trace element ratios vs. oxides (Al2O3/P2O5) in marine sediments of the world (Planke, 2005). Polygons show typical ratios in lithologic units or tectonic regions; stars refer to average compositions obtained in sediments accumulated in pits; circles with letters indicate ratios obtained in compositional averages of continental crust (A and C), global sediments in subduction (B) and shales of post-Archean age (D); dark green squares refer to contents found in sediments obtained from diapirs in northern Colombia. Map in the right side show the location of mud volcanic samples and their Th/La ratio (diameters of the circles refer to the ratio obtained), grouped by families according to the trends observed in the graph on the left side (sediments derived from granitic sources - acid volcanics, or from varied volcanic sources).

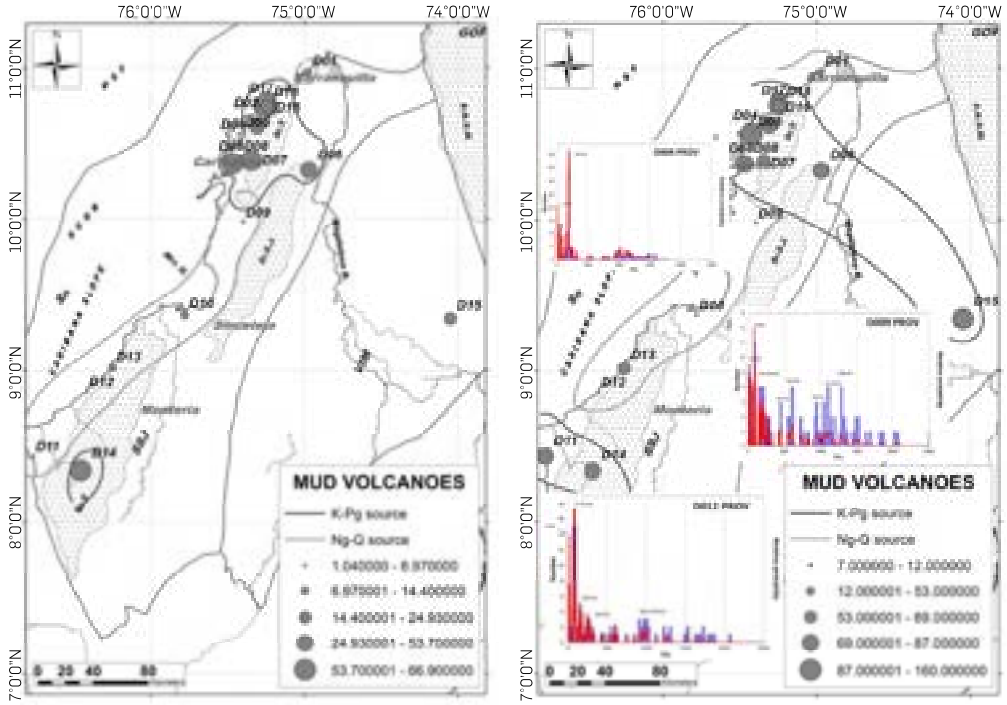

Figure 6. Left side map of the location of mud volcano samples and the age of the youngest grain obtained in each one (diameter of the circles refers to the age in Ma). Note the concentration of ages older than 24 Ma in the northern part of the studied area (surrounded by the thick dark gray line), while ages younger than 14 Ma appear to be concentrated in mud volcanoes located in the central and southern part of the study area (surrounded by the light gray line). Right side map of location of mud volcano samples and the age of the youngest zircon population obtained in each (diameter of circles refers to age in Ma). Note the concentration of ages older than 69 Ma in the northern and southern part of the study area (surrounded by the thick dark gray line) and examples of relative probability vs Ma plot for U/Pb ages plots from samples of the Flamenco and Yerbabuena mud volcanoes (D004 and 009), while ages younger than 53 Ma appear to be concentrated in the central part of the study area (mud volcanoes surrounded by the light gray line) and example of probability vs Ma plot for U/Pb ages plot obtained from samples of the Arboletes mud volcano (D012).

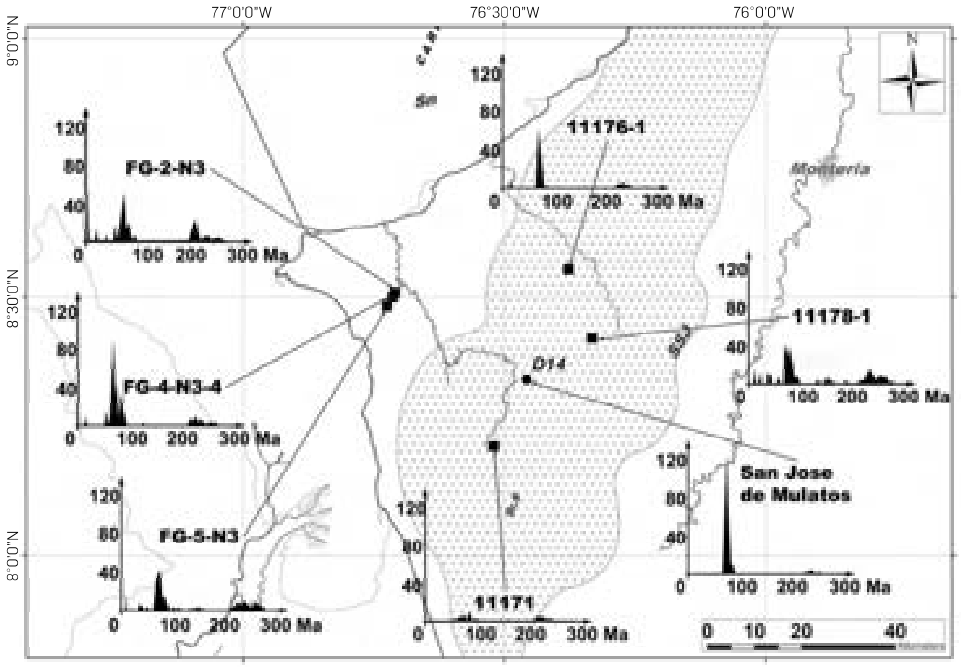

Figure 7. Location map of the San Jose de Mulatos mud volcano, samples from nearby outcrops and the relative frequency diagrams of number of zircon grains vs. age plots for the 0 to 300 Ma interval result of the U/Pb analysis. Note the similarity of the 70 to 80 Ma and 250 to 300 Ma ages recovered from the mud volcano and surrounding units.

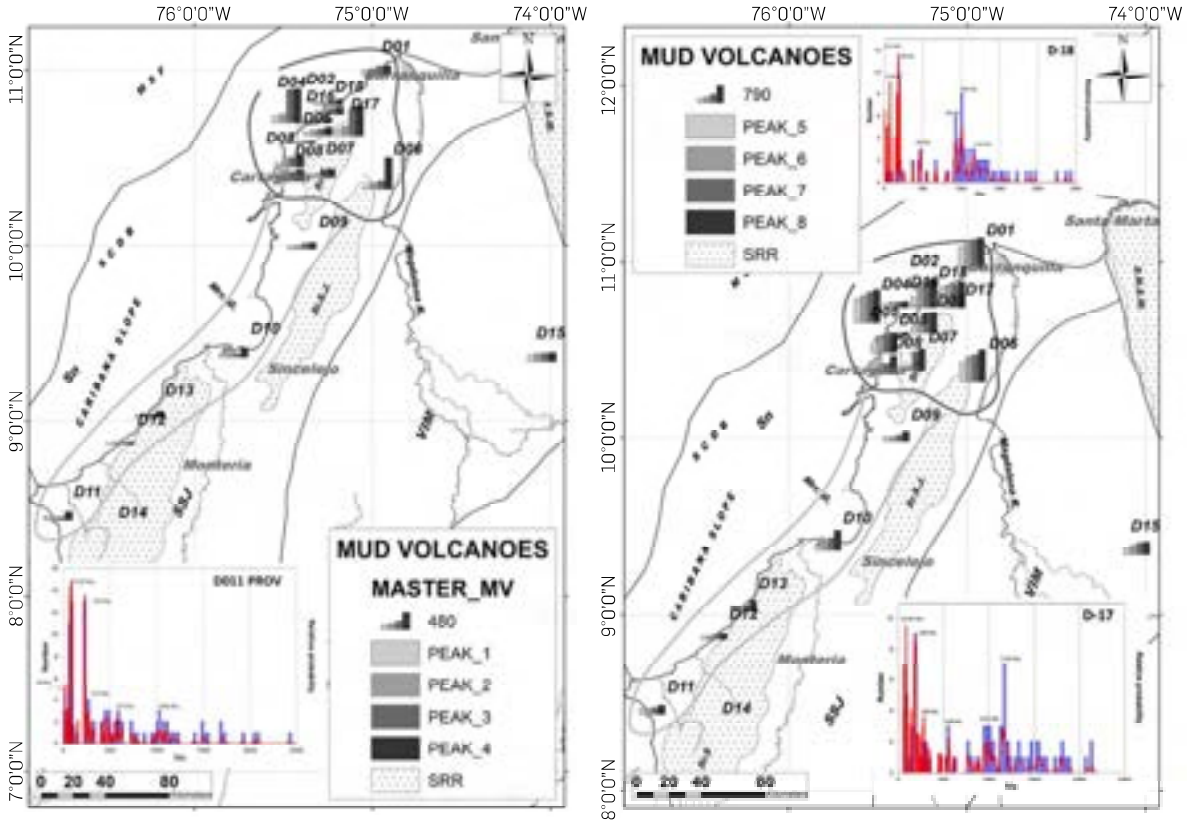

Figure 8. Maps of mud volcanoes location and U/Pb ages of the 4 youngest zircon grain populations (left side) and 4 oldest zircon grain populations (right side), obtained from each sampled mud (bar length refers to millions of years recorded by population, maximum recorded 480 Ma for populations on the left and 790 Ma for populations on the right). Note the concentration of ages younger than 100 Ma in the Sinú - San Jacinto Basin (SSJ) and west of the Serranía de San Jacinto (Sr.S.J.) surrounded by the light gray thick line, while ages older than 100 Ma seem to be concentrated in the mudstones of the volcanoes located in the Serranía de Tubará (Sr.T.) and north of Serranía de San Jacinto (Sr.S.J.), surrounded by the dark gray thick line. Examples of probability vs Ma plots for U/Pb ages obtained in the mud volcanoes Virgen del Cobre (D011), Totumo and Vía al Totumo (D17 and 18)

al., 2011; Lara *et al*., 2013; Gómez *et al*., 2015; Silva-Arias *et al*., 2016; León *et al*., 2018; Jaramillo *et al*., 2019; López-Ramos *et al*., 2021) and the database "Map of uranium lead chronology samples from basement and detrital samples", a consolidated database managed by the ICP (Instituto Colombiano del Petróleo). The ninety U/Pb age values in detrital zircons were discriminated according to the age of the formation from which the samples were extracted into: Cretaceous (13 samples); Upper Paleocene - Lower Eocene (30 samples); Middle to Upper Eocene (20 samples); Oligocene (8 samples); Miocene - Pliocene (20 samples). The results of the selection were represented in the form of relative frequency diagrams, trying to reproduce the behaviour of the U/Pb ages of the detrital zircons recovered in the sampled sedimentary sequences (Figure 9). Similar diagrams were created for the results obtained in the mud volcano samples, which were compared with the diagrams of the sedimentary sequences analyzed to select, based on the best match between diagrams, the probable stratigraphic level of detachment of the mud volcanoes. From the comparative analysis, it is observed that the mud volcanoes can be grouped into four groups, indicative of stratigraphic detachments levels with different ages (Figure 9).

Group 1 of mud diapirs: U/Pb ages of detrital zircon grains recovered from sedimentary units accumulated during the late Paleocene - early Eocene (San Cayetano Fm.), show three main population ranges (Figure 9): one between 80 and 130 My (Cretaceous); another between 210 and 300 My (Permo - Triassic); a third between 500 and 1,000 My (Mesoproterozoic - Cambrian). Two of the three population age ranges described above for sedimentary units accumulated from the late Paleocene - early Eocene coincide with the population age ranges obtained from zircons recovered from mud samples taken from the Cañaveral mud volcano, south of the Serranía de Tubará (Figure 9). This coincidence suggests that the analyzed muds from the Canaveral mud volcano may have as a detachment level, sediments accumulated from the late Paleocene to early Eocene.

Group 2 of mud diapirs: The sedimentary units accumulated during the middle - late Eocene (Maco, Chengue and San Jacinto formations), which rest discordantly over sedimentary units of the late Paleocene - early Eocene (San Cayetano Formation), contain detrital zircons, whose U/Pb ages can be grouped into three population ranges (Figure 9): one between 65 and 90 My (Late Cretaceous); other with ages between 180 and 320 My (Permo-Triassic); a third population with ages between 510 and 970 My (Neoproterozoic - Cambrian). These three age populations are also present in detrital zircons analyzed by the U/Pb method from mud volcanoes such as El Rodeo (Central and Lateral) located southwest of the Serranía de Tubará and Santa Lucía to the north of the Serranía de San Jacinto. This coincidence suggests that the mudstones from El Rodeo (Central and Lateral) and Santa Lucía mud volcanoes are derived from sedimentary sequences accumulated from the middle - late Eocene (Figure 9).

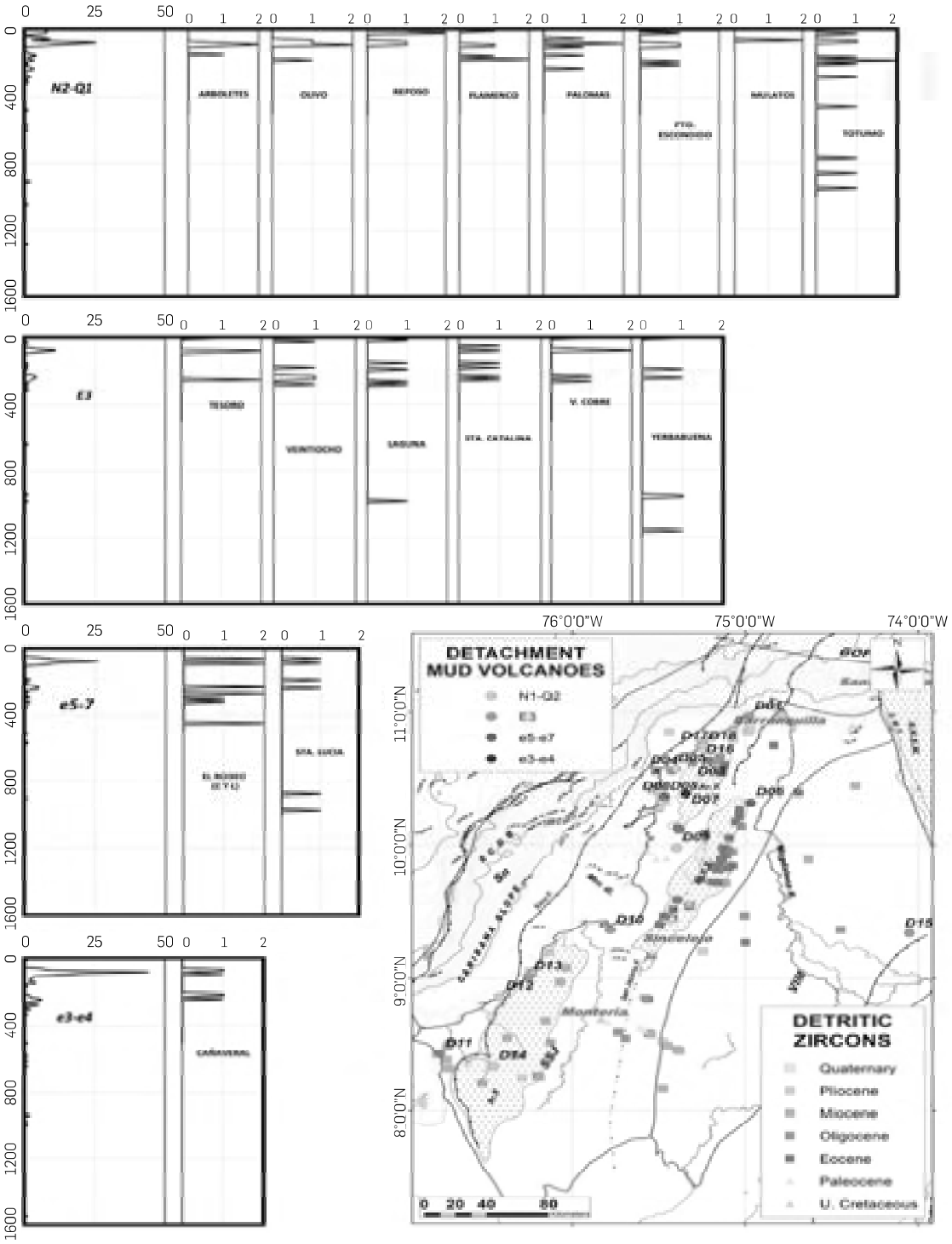

Figure 9. Age plots of the 4 youngest populations of detrital zircons, obtained in sedimentary sequences accumulated in the Lower Magdalena (VIM) and Sinú - San Jacinto (SSJ) basins in the left column, and in samples recovered from the studied mud volcanoes in the right columns, grouped according to similarity of the ages of the e3-e4 zircon populations: Late Paleocene to early Eocene (Cañaveral volcano); e5-e7: Middle to late Eocene (El Rodeo and Santa Lucia volcanoes); E3: Oligocene (volcanoes El Tesoro, El Veintiocho, La Laguna, Santa Catalina, Virgen del Cobre and Yerbabuena); N1 - Q2: Miocene to Quaternary (volcanoes Arboletes, Olivo, Reposo, Flmanco, Palomas, Puerto Escondido, Mulatos, El Totumo). Location of mud volcanoes classified according to their possible stratigraphic detachment level (map in the bottom right side) and location of samples with ages obtained through analysis of detrital zircons, using U/Pb technique from published works (Villagómez Díaz, 2010; Cardona et al., 2012; Lara et al., 2013; J. Gómez et al., 2015; León et al., 2018) and own analysis of this project.

Group 3 of mud diapirs: The detrital zircons extracted from sedimentary formations accumulated during the Oligocene (Cienaga de Oro and Carmen shale), show three main U/Pb age populations: one population between 75 and 85 My (Late Cretaceous); another population between 150 and 280 My (Permo-Traissic); a third population with values ranging between 640 and 980 My (Neoproterozoic). These three populations of zircon ages coincide with those obtained from zircons recovered from mud volcanoes such as El Tesoro (north of the Serranía del Sinú), El Veintiocho (central part of the Lower Magdalena Basin), La Laguna (north of the Serranía de Tubará), Santa Catalina (western flank of the Serranía de Tubará), Virgen del Cobre (south of the Serranía del Sinú), and Yerbabuena (western flank of the Serranía de Tubará). This coincidence suggests that the mud expelled by these mud volcanoes may be detached from sedimentary sequences of Oligocene age (Figure 9).

Group 4 of mud diapirs: The sedimentary formations accumulated during the Miocene and Quaternary in the area of Serranía de San Jacinto, Serranía del Sinú, and Serranía de Tubará (correspond with the Campano, Pavo, Floresanto, Pajuil, Moñitos, Morrocoy - El Pantano, Arenas Monas, Borqueles, Porquero, Sincelejo and Betulia formations), contain detrital zircons with ages that allow defining three main populations: a population of very young zircons, with values between 5 and 90 My (Late Cretaceous - Late Miocene); a second population of zircons with ages between 160 and 230 My (Permo-Triassic); a third population of zircons with ages between 315 and 915 My (Early Carboniferous - Neoproterozoic). The ages of zircons recovered in samples from mud volcanoes such as Arboletes - Puerto Escondido (western flank of Serranía del Sinú), San José de Mulatos (central part of the Serranía del Sinú), El Olivo - El Reposo - Flamento (western flank of the Serranía de Tubará) and Las Palomas - El Totumo - via El Totumo (north of the Serranía de Tubará), coincide with the age ranges defined in the three age populations defined in the sedimentary sequences accumulated during the Neogene in the study area. This suggests that these mud volcanoes, detached from sedimentary sequences, accumulated during the Neogene (Figure 9).

MICROPALEONTOLOGICAL AND PALYNOLOGICAL AGES

Samples collected from mud volcanoes contain foraminifera (planktonic and benthic) and palynomorphs that, like zircons, were dragged during the intrusion of the mud to the surface through sedimentary sequences. Thus, the ages inferred by the presence of these foraminifera and palynomorphs reflect the age of the sedimentary sequences crossed by the mud to the surface, and compare with the ages of the mud volcano clusters previously discussed in the analysis by coincident clustering of U/Pb age populations in detrital zircons.

Of the 18 volcanoes analyzed, 14 showed sufficient recovery for dating by planktonic foraminifera, and 6 samples show a recovery mostly of benthic foraminifera. Preservation of planktonic foraminifera is fair to good, with low percentages of broken, deformed or pyritized shells; only one sample (Santa Catalina volcano) has a high percentage of deformed shells. The preservation of benthic foraminifera is fair to good, with low percentages of broken, deformed or pyritized shells. The planktonic foraminifera recovered suggest that the Totumo volcano muds contain Plio-Pleistocene age faunas, while volcanoes such as El Reposo, Yerbabuena, and San José de Mulatos contain faunas of middle to late Miocene age (Figure 10). Other volcanoes such as Virgen del Cobre, Arboletes, Santa Catalina, El Tesoro, El Rodeo (central), and Puerto Escondido contain planktonic foraminiferal faunas in their muds, predominantly of early to middle Miocene age (Figure 10). Samples from El Rodeo (lateral) and La Laguna volcanoes contain planktonic foraminiferal faunas of Oligocene age, while Santa Lucía and Olivo volcanoes

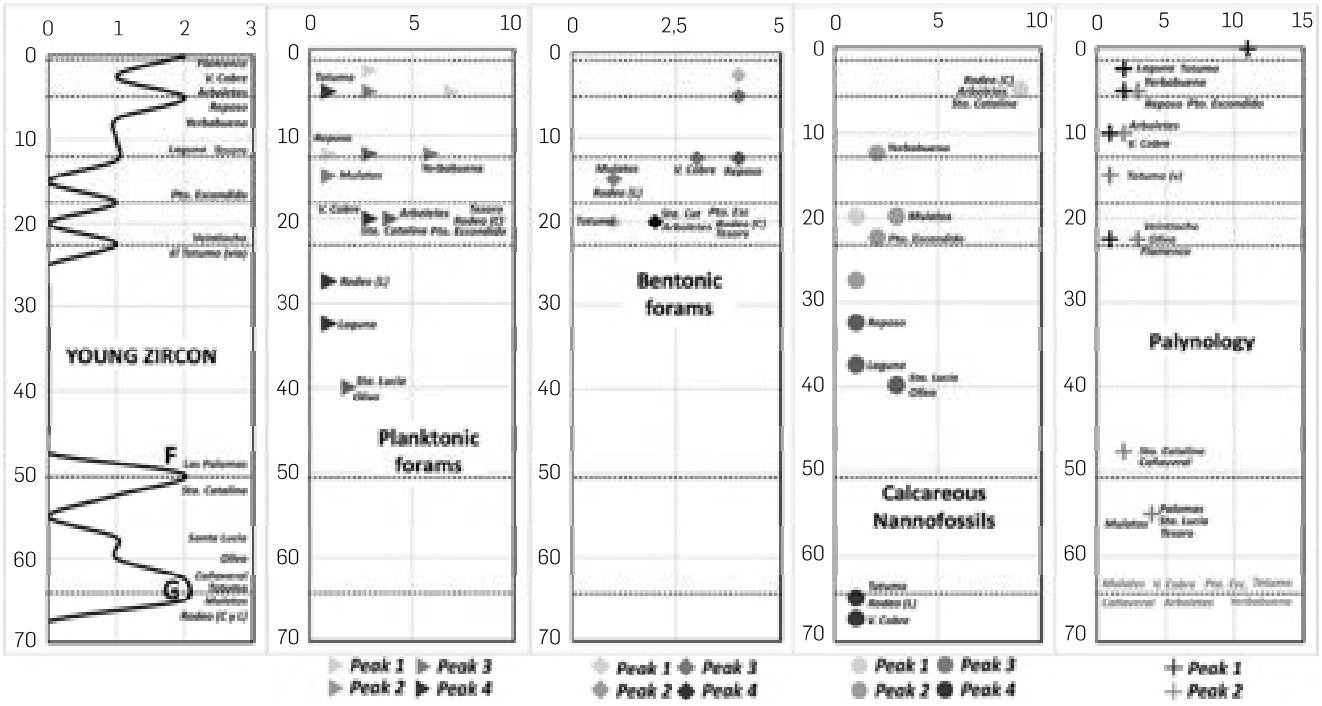

Figure 10. Graph of ages of younger zircon recovered in samples from the mud volcanoes studied (left column). Ages of planktonic foraminiferal, benthic, nannofossil and palynological faunal peaks recovered from sampled mud volcano samples (Rigth columns).

have faunas of Eocene age (Figure 10). The benthic foraminiferal faunas from Virgen del Cobre, El Reposo, San José de Mulatos, El Rodeo (Central and Lateral), El Totumo, Santa Catalina, Arboletes, El Tesoro, and Puerto Escondido volcanoes show predominantly early to middle Miocene ages (Figure 10). The analysis of calcareous nannofossils shows faunas of predominantly Plio-Pleistocene ages in volcanoes such as El Rodeo (Central), Arboletes, and Santa Catalina, while in volcanoes such as Yerbabuena, San José de Mulatos, and Puerto Escondido, they show predominantly Miocene ages (Figure 10). Volcanoes such as El Reposo, La Laguna, Santa Lucía, and El Olivo, show faunas of Eocene-Oligocene age, while in volcanoes such as El Rodeo (Lateral) and Virgen del Cobre, faunas of Cretaceous age were recovered (Figure 10).

Of the 22 diapir samples analyzed, 3 samples were sterile in palynomorphs (Santa Lucía and El Rodeo Lateral - Central). Considering the oldest record of pollen recorded in each mud volcano, it is observed that volcanoes such as Las Palomas, Santa Catalina, Santa Lucía, Cañaveral, El Tesoro, and San José de Mulatos, may be transporting mud from Paleocene - Eocene sequences (Figure 10), while volcanoes such as Flamenco, El Veintiocho, and El Olivo transport muds from the Lower Miocene (Figure 10). Volcanoes such as Arboletes, Virgen del Cobre, and Vía al Totumo, present palynological records suggesting contributions from upper Miocene units, while volcanoes such as Yerbabuena and El Reposo are from the upper Miocene (Figure 10). Pliocene palynological records are present in volcanoes such as La Laguna and El Totumo (Figure 10). Samples from volcanoes such as Virgen del Cobre, Yerbabuena, Cañaveral, Arboletes, Puerto Escondido, El Totumo (road and volcano), and San José de Mulatos, show Cretaceous-Paleocene palynomorphs (Figure 10).

WATER GEOCHEMISTRY

Water samples extracted from mud volcanoes were subjected to geochemical (anions and cations) and isotopic ($\delta^{18}O$ y δD) analyses to determine their diagenetic or meteoric origin (Table 5). Water samples taken from marshes, rivers, coast and salt dewatering ponds were used to establish a local meteoric water line to then contrast it with the global meteoric line (Figure 11). The relationship between $\delta^{18}O$ vs δD values of water recovered from mud volcanoes (at active taps) tends to be linearly negative, except for Las Palomas and Virgen del Cobre volcanoes, which show a marked trend toward the local meteoric water baseline (Figure 11). The range of $\delta^{18}O$ values in volcanoes showing a linear relationship varies between 0 and 8,

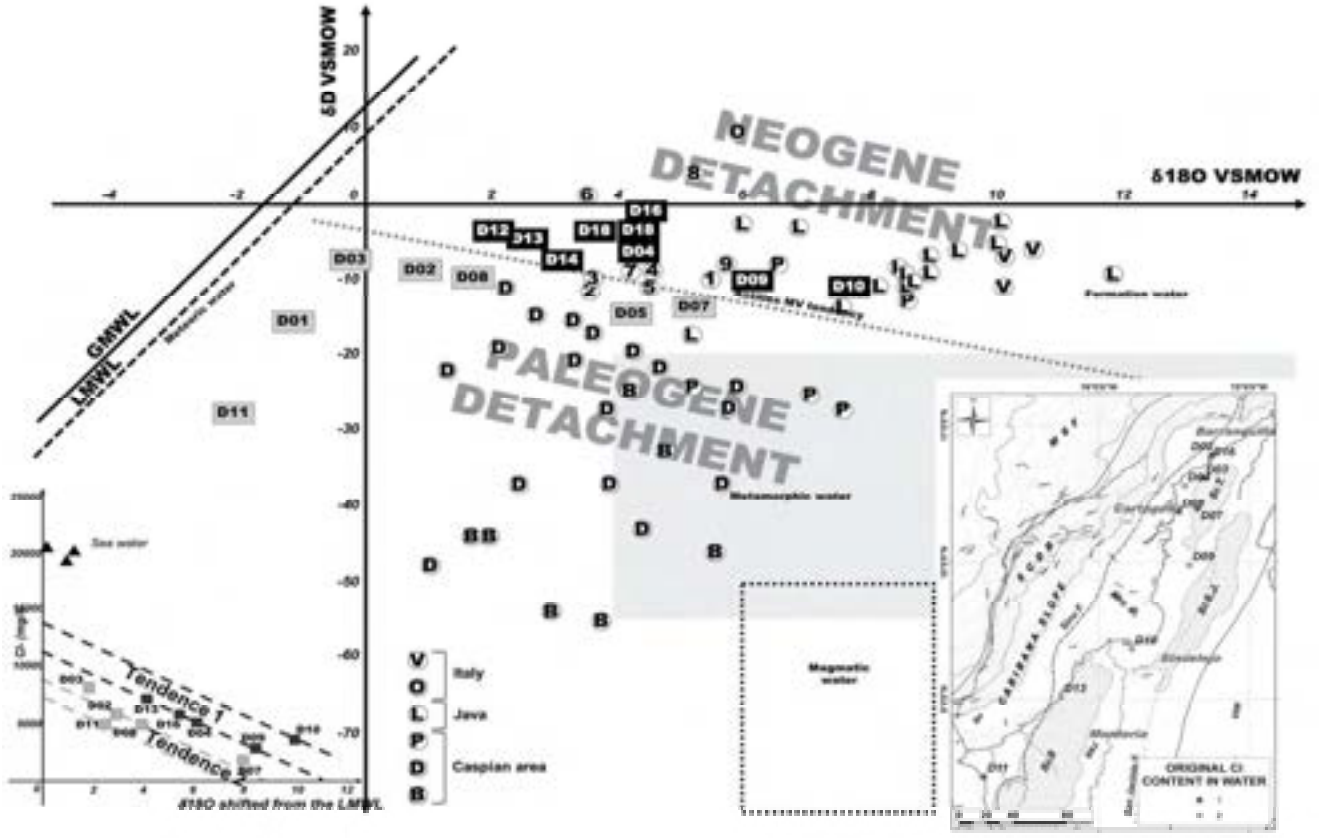

Figure 11. Isotopic $\delta^{18}O$ vs δD correlation of water samples recovered from Colombian Caribbean mud volcanoes (center) and their relationship to similar isotopic analyses at other mud volcanoes in the southern Caspian Basin (P, D, B), Java (L), Italy (V, O), Antilles (trend line) and Colombian Caribbean (numbers 1 to 9 in circles), compiled from various studies (Geoffroy, 2005; Madonia et al., 2011; Agustawijaya et al., 2017; Mazzini and Etiope, 2017; di Luccio et al., 2021). Note the families of mud volcanoes in the Caribbean of Colombia, according to their position above (trend 1 defined by mud volcanoes in black box), or below (trend 2 defined by mud volcanoes in gray box) the regional trend of Antillean mud volcanoes. On the left, the same trends expressed by the relationship between the difference in stable δ18O isotope values and the Local Meteoric Water Baseline (LMWL) and Cl- content in mg/l, where dashed black lines refer to trend 1 of mud volcanoes with high initial Cl- content (black squares in the diagram and map), and the dashed gray lines refer to trend 2 of mud volcanoes with low initial Cl content (gray squares in the diagram and map). Data source are recorded in Table 5 for the mud volcanoes sampled during this work.

while δD varies between 0 and -20 (Figure 11). The isotopic analyses of water samples obtained from mud volcanoes were compared with global and local trend lines of meteoric water, which allowed us to identify their offset as a function of $\delta^{18}O$ (Figure 11). The isotopic lag obtained between the local meteoric water line and each water sample recovered from the mud volcanoes was compared with the Cl- anion content, showing two negative linear trends (trends 1 and 2), as the $\delta^{18}O$ isotopic lag value increases with respect to the local meteoric water line, while the Cl- concentration decreases (Figure 11). Trend 1 is formed by volcanoes such as Santa Catalina, Virgen del Cobre, Las Palomas, El Rodeo, and Cañaveral, where the initial chloride concentration before expelling diagenetic waters (value projected to the $\delta^{18}O$, isotopic lag value of zero), varies between 12000 and 14000 mg/l (Figure 11). Trend 2, formed by volcanoes such as Puerto Escondido, El Olivo, Yerbabuena, Flamenco, and El Tesoro, is characterized by initial chloride concentrations between 8,500 and 7,000 mg/l before expelling diagenetic waters.

MOLECULAR AND ISOTOPIC COMPOSITION OF NATURAL GAS

From the compositional results of the 14 mud volcanoes sampled, 10 volcanoes showed significant values of gases associated with thermogenic processes (Figure 12): La Laguna, Las Palomas, Santa Catalina, Yerbabuena, El Reposo, Cañaveral, El Rodeo, Flamenco, Virgen del Cobre, and Puerto Escondido. The major element composition of the hydrocarbon-associated gases in these samples is largely dominated by methane, with a significant CO_2 content. In contrast, samples from the Santa Lucía, El Tesoro, Arboletes, and San José de Mulatos volcanoes showed low concentration of hydrocarbons, and an overall composition of N_2 77.9% and O_2 21.8%, values very close to the compositional reference for atmospheric gases (Figure 12). The results of the main element composition of the natural gases show a higher concentration of methane, which may be related to the fractionation of hydrocarbons during the vertical migration process. Therefore, the gas analyses focus on the isotopy that was measured especially in methane and CO_2. At large, methane is the gaseous compound found in the highest percentage, above 80%, followed by non-hydrocarbon gases such as carbon dioxide (CO_2), nitrogen (N_2), and some other elements in smaller proportions such as C_2-C_5 and noble gases, mainly He. Methane can be produced by thermal cracking processes of organic matter at temperatures above 100ºC or it can be generated, in a less studied process, by microbial activity using CO_2 reduction or acetate fermentation as the mechanism to generate this methane (Milkov and Etiope, 2018). The results obtained show a wide range of origins and processes involved in the emanation of this natural gas through the mud diapir. In four of the samples, an origin associated with the primary microbial activity is suggested (El Reposo, Las Palomas, Yerbabuena, and El Rodeo volcanoes), with $\delta_{13}C_1$ values between -65 and -60‰ and negative CO_2 values (Figure 12). In three of the samples (Santa Catalina,

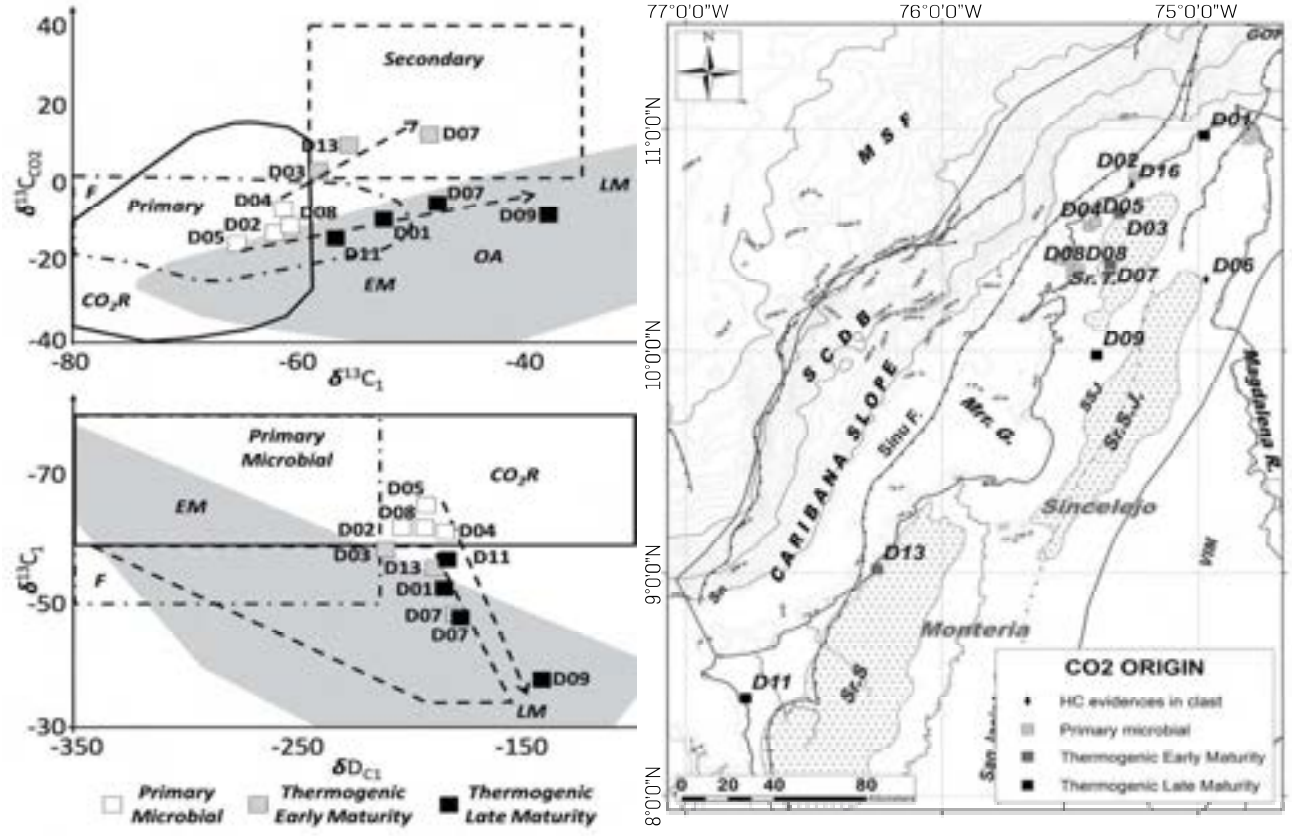

Figure 12. Left upper diagram $\delta^{13}C_1$ vs $\delta^{13}C_{CO_2}$, bottom diagram $\delta^{13}C_1$ vs δ_{DC_1}, and their relationship to CO_2 generation (Milkov and Etiope, 2018). Primary microbial natural gas, generated by the activity on an organic precursor of the source rock by: F= Fermentation or by CO_2; R= CO_2 reduction. Thermogenic natural gas of different stages of maturity: EM= early maturity gas; OA= gases associated with an oil; LM= gases associated with a late maturity. Volcanoes: 1= La Laguna; 2= Las Palomas; 3= Santa Catalina; 4= Yerbabuena; 5= El Reposo; 7= Cañaveral; 8= El Rodeo; 9= Flamenco; 11= Virgen del Cobre; 13= Puerto Escondido. Right, distribution map of mud volcanoes and their classification according to CO_2 isotopic origin analysis. Data sources are recorded in Table 6 for the mud volcanoes sampled during this work.

Puerto Escondido, and Cañaveral mud volcanoes), a thermogenic origin is suggested to an early maturation window, with the addition of secondary microbial gases (Milkov, 2011, 2018), given $\delta_{13}C_1$ values between -60 and -45‰, as well as positive CO_2 values (Figure 12). A clear example of these processes is that of the Cañaveral volcano, where two samples from the same volcano, extracted from different emanation centers, have the same thermal maturity with different biodegradation processes. The samples from Virgen del Cobre, La Laguna, Cañaveral, and Flamenco volcanoes show a clear linear maturity trend, until reaching the middle methane gas window, associated with oil, in a late maturity stage until the beginning of the gas generation window (Figure 12), reflecting the degree of maturity of the source rock producing this methane.

DISTRIBUTION OF MUD VOLCANISM AND THEIR MORPHOLOGY IN THE COLOMBIAN CARIBBEAN

Mud volcanism in the Colombian Caribbean has a wide distribution in the maritime and continental domains. The compilation of geological and geomorphological cartographic data in the continental domain (Guzman *et al.*, 1998; Reyes, *et al.*, 1998; Barrera, 2001; Clavijo and Barrera, 2002; Geotec Ltda., 2003; Guzman, et al., 2003; ANH, 2005; Carvajal and Mendivelso, 2017), allows estimating the presence of more than 80 identified mud volcanoes, which may be higher, considering the dense vegetation by sectors in northern Colombia, while in the maritime domain, geological and bathymetric research works (Shepard, et al., 1968; Aristizábal, et al., 2009; Domínguez *et al.*, 2010; Quintero, 2012; Bernal-Olaya, Mann and Vargas, 2016; Herrera Atencio and Díaz Mendoza, 2018; Rincón Martínez *et al.*, 2021), together with available seismic information, suggest the presence of more than 200 mud volcanoes (Figure 1). The inventory of mud volcanoes shows that, despite their large number, their distribution in northern Colombia is not homogeneous, differentiating 4 large blocks according to their occurrence per 25 km² (Figure 1), each one with different extensions, heights and ellipticities (Table 4):

Block 1 of mud volcanoes: This block is located along the Serranía del Sinú and the southern part of the Sinú offshore basin, occupying an area of approximately 10,000 km² (Figure 2 and Table 4). The presence of mud volcanoes in this block tends to be low (0.009 mud volcanoes/25 km²), with an average area per mud volcano of 3.59 km², with average ellipticity values of 15% (slightly elliptical) and morphologically prominent over the terrain, averaging 118 m (Table 4).

Table 4. Main morphological characteristics of the mud volcanoes (MV) that compose the four blocks with the highest number of volcanoes by 25km² cells (see blocks distribution in Figure 1).

PARAMETER		Block 1	Block 2	Block 3	Block 4
BLOCK AREA km²		10000	17300	11200	8100
NUMBER OF MV/25 km²		0,009	0,07	0,025	0,025
AREA km²	MAX	24,81	30,73	20,98	26,55
	MIN	0,13	0,21	0,35	0,17
	MEAN	3,59	1,45	2,8	5,1
	DESV. EST	5,23	9,09	4,84	6,45
ELIPTICITY %	MAX	37	56	62	51
	MIN	0,05	0,03	0,03	0,02
	MEAN	15	25	23	16
	DESV. ESTMAX	11	17	13	16
HEIGHT m	MAX	426	238	400	342
	MIN	11	20	6	3
	MEAN	118	116	149	71
	DESV. ES	99	65	65	73

Block 2 of mud volcanoes: The extension of this block is 17,300 km² (the largest area affected by mud volcanoes in the Colombian Caribbean), covering the northern part of the Sinú offshore basin, north of the Serranía del Sinú and the western flank of the Serranía de Tubará (Figure 1 and Table 4). This block shows the highest presence of mud volcanoes in the studied area (0.07 volcanoes/25km²), with average areas per mud volcano of 1.45 km² (relatively small), average ellipticity of 25% (significant ellipticity) and heights above ground averaging 116 m (similar to those of block 1).

Block 3 of mud volcanoes: With an extension similar to that of block

Table 5. Data of isotopic $\delta^{18}O$ vs δD in water samples recovered from Colombian Caribbean mud volcanoes for this work (see Figure 11 for graphic relationships). The mud volcanoes column refers to the number of the analized mud volcano (Names of mud volcanoes in Tables 2 and 3 and location in Figure 1).

Cl- mg/l	dD	d18O	Shift Isotopos	HF Mw/M2	IC	CC	HL/Sm1	HL/Sm2	MUD VOLCANOES
1,46	-16	-1,1	2	82	0,6	0,3	10	75	1
5864,00	-9	0,87	3,1	48	0,8	0,3	10	65	2
8122,00	-8	-0,21	1,9	24	0,7	0,3	20	75	3
5142,00	-6,3	4,32	6,3	20	1	0,3	20	75	4
4042,00	-14	4,19	7,1	20	0,5	0,3	25	75	5
				24	0,7	0,3	35	75	6
1706,00	-13	-0,18	8	20	0,4	0,4	20	65	7
	-9,3	1,69	4	20	0,6	0,3	30	70	8
5085,00	-9,7	6,13	4	20	0,5	0,3	20	75	8
2925,00	-11	7,67	8,4	25	0,5	0,3	20	75	9
3847,00	-28	-2,06	10,1	31	0,6	0,3	15	70	10
5001,00	-3,4	2,07	3,5	49	0,6	0,3			11
7274,00	-4,1	2,56	4	42	0,5	0,3	30	75	12
112,00	-7,3	3,12	5	56	0,6	0,4	40	75	13

1 of mud volcanoes (11,200 km^2), it is located in the southern and central part of the Guajira offshore basin and the northern part of the Serranía de Tubará (Figure 1 and Table 4), with an intermediate occurrence of mud volcanoes (0.025 mud volcanoes/25 km^2), with an average area per mud volcano of 2.8 km^2 (relatively small), average ellipticity of 23% (significant ellipticity), and heights above ground averaging 149 m.

Block 4 of mud volcanoes: This block is located north of the Guajira Peninsula, in the offshore domain, with an area of 8,100 km^2 (Figure 1 and Table 4), with a similar occurrence of mud volcanoes to those recorded in Block 3 (0.025 mud volcanoes/25 km^2), characterized by mud volcano buildings with large areas (5.1 km^2 on average), mean ellipticity values of 16% (slightly elliptical), and heights above the ground averaging 71 m.

5. DISCUSSION

CLAY MINERALOGY, OXIDE, AND TRACE ELEMENT CONCENTRATIONS AS INDICATORS OF PROVENANCE OF SEDIMENTARY SEQUENCE'S CROSSED BY MUD VOLCANOES

The results of compositional analysis of the total minerals and XRD in clays, suggest the presence of two families of mud volcanoes (Figures 3 and 13): Family one, located along the Serranía del Sinú, in which the Chlorite fraction is predominant, low crystallinity indexes in Illite and high crystallinity indexes in Kaolinite (varies between 0.3 to 0.4 Δ °2θ); Family two, located along the Serranía de San Jacinto, Serranía de Tubará, and the VIM basin, in which Smectite predominates, Chlorite fraction decreases, the index of Illite crystallinity increases, and the Kaolinite crystallinity indexes (up to 0.15 Δ °2θ) decrease. The crystallinity index in Ilites is commonly used as an indicator of incipient metamorphism, decreasing its crystallinity as metamorphism increases (Clauer and Chaudhuri, 1995; Jaboyedoff *et al.*, 2001), as well as the presence of Chlorite that can be interpreted as a result of deep diagenetic processes - incipient metamorphic, detrital from metamorphic sources or by alteration of mafic minerals such as pyroxene and olivine (Hillier, 1993; Clauer and Chaudhuri, 1995; Wu *et al.*, 2019; Fulignati, 2020). The increase in the crystallinity index of kaolinite has been considered an indicator of its origin linked to alteration processes under high-temperature conditions (e.g. hydrothermal), while its decrease suggests an origin linked to weathering processes (Oluwadebi, 2015; Saha, Reza and Roy, 2020).

In the Cenozoic sedimentary sequences outcropping in the Serranía del Sinú, as well as those drilled by exploratory hydrocarbon wells in the VIM basin, no low-grade metamorphism or sedimentary rocks affected by deep diagenetic processes have been reported. However, the presence of conglomeratic levels is frequent, especially from formations accumulated at the end of the Paleocene (San Cayetano Fm.) and during the Eocene (Maco, Chengue and San Jacinto formations), which are rich in pebbles and cobbles of igneous rocks of variable composition and degree of alteration, as well as low-grade metamorphic rocks (Cardona *et al.*, 2012; Silva-Arias *et al.*, 2016; J. Mora *et al.*, 2018). Therefore, considerate is likely that the high contents of Chlorite and Ilite with a low degree of crystallization, and high crystallization indexes of Kaolinite, present in the mud volcanoes sampled along the Serranía del Sinú (Family one), come from Cenozoic sedimentary sequences rich in these clay minerals in detrital form. Isotopic analyses on gases such as CO_2 recovered from the different mud volcanoes analyzed along the Serranía del Sinú show a clear mixture of gases of microbial to early thermogenic origin (Figure 12), consistent with the low degree of maturity of the organic matter recovered from the drilling of exploratory wells (Aguilera, 2011). Thus, it can be suggested that the Chlorite and Ilite with a low degree of crystallinity present in the volcanic muds of the Serranía del Sinú, and the high crystallinity index of Kaolinite (Family one) have not been the result of deep diagenetic processes, incipient metamorphism of the formations crossed by the volcanic muds or hydrothermal activity, but reflect the composition of the detritus accumulated during the Cenozoic in the area from metamorphic or igneous sources rich in pyroxenes and amphiboles, little altered, common lithologies in the edges of the Cauca - Patía basin (Central and Western Cordilleras). The same process of mud dragging is suggested for the area of mud volcanoes located along the Serranía de San Jacinto and Serranía de Tubará (Family two), but the decrease in Chlorite, the increase in the degree of crystallinity of Ilite, and the low crystallinity indexes of the Kaolinite, suggest that the detritus accumulated during the Cenozoic in those areas, came from massifs exposed to weathering, poor in pyroxenes and amphiboles. Analyses of clay minerals extracted from El Totumo volcano, show that kaolinite and its varieties, have not undergone burial processes greater than 1 km (Dill and Kaufhold, 2018), suggesting that the detachment rock is not very deep (probably Miocene).

Other clay minerals extracted from the samples of mud volcanoes in the northern part of the Serranía de San Jacinto, Serranía de Tubará and VIM basin (Family Two) are Montmorillonite and Beidelite. The presence of Montmorillonite is considered an indicator of volcanic or hydrothermal weathered sediment sources (Yamada *et al.*, 1991); however, the presence of Beidelite is rarer, mainly associated with mica alteration (Fesharaki *et al.*, 2007). Thus, it can be considered that the mud expelled by the mud volcanoes in the northern part of Serranía de San Jacinto, Serranía de Tubará and VIM basin (Family two), crossed and dragged sedimentary sequences with detritus from areas composed of altered volcanic or metamorphic rocks, such as those exposed in the Santander cratonic massifs and along the Cordillera Central. This is consistent with the significant smectite values recorded in Family Two of mud volcanoes (Figure 3), as well as along the Upper Magdalena Valley, in sediments of the Honda Fm, which reflect the high input of sediments from active igneous volcanic centers, developed during the Miocene along the Cordillera Central (Laguna *et al.*, 2008). The oxide concentration ratios in the analyzed mud samples as TiO_2 and Al_2O_3 (Figure 4), seem to confirm the grouping of mud volcanics into the two families discussed above. Thus, TiO_2 concentrations tend to be higher than Al_2O_3 concentrations in the mud volcanics along the Serranía del Sinú (Family one), while it tends to be reversed in the mud volcanics sampled in the northern part of the Serranía de San Jacinto, Serranía de Tubará, and VIM basin (Family two). On the other hand, the ratios of trace element concentrations such as Th/Co and La/Sc (Figure 4), tend to be low in the mud volcanoes along the Serranía del Sinú (Family one), while they increase in the mud volcanoes along the Serranía de San Jacinto, Serranía de Tubará, and VIM basin (Family two). Comparison of oxide ratios and trace element concentrations obtained in this work, with geochemical characterization studies of clays (Amajor, 1987; El-Wekeil and El-Anwar, 2013; Chen *et al.*, 2016; Mitra, et al., 2018), suggest that TiO_2 vs Al_2O_3 and Th/Co vs La/Sc ratios are similar to those observed in Family One mud volcanoes, are characteristic of sediments from source areas composed of basaltic rocks, whereas ratios similar to those observed in Family two mud volcanoes suggest sediment sources from areas composed mainly of granitic rocks (Figure 4). Global studies of the Th/Lt ratio in marine sediments and basaltic arcs (Planke, 2005) suggest that

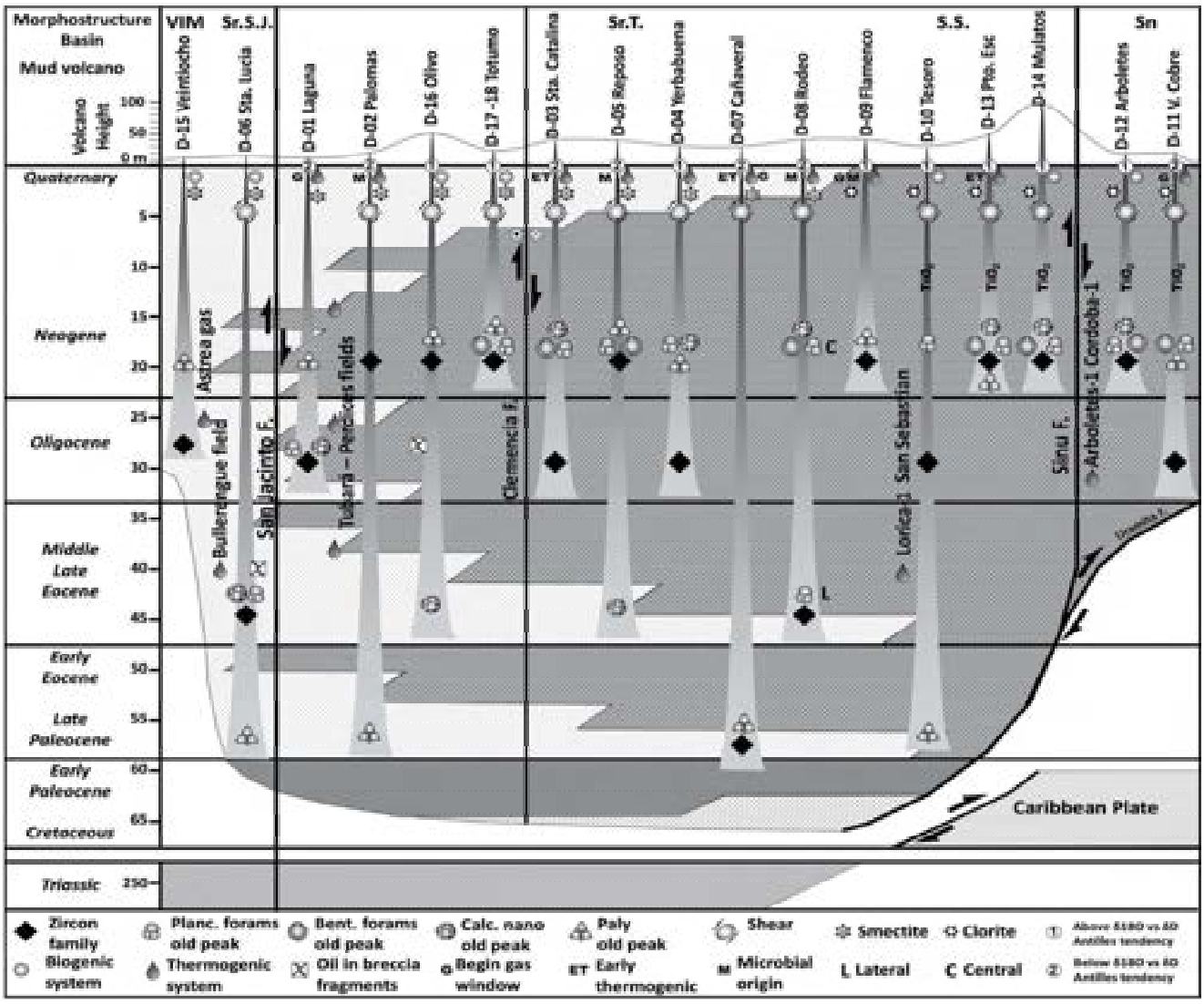

Figure 13. Chronostratigraphic sketch of possible detachment levels of the mud ejected by the mud volcanoes studied in the Colombian Caribbean (left column refer to the chronostratigraphic time scale), based on the recoveries of detrital zircon families (outcropping formations in the area and recovered from the mud volcanoes) and microfauna's (planktonic, benthic, nannofossils and pollen). The results obtained in the analysis of relevant clay minerals, evidence of gas-oil and its origin, deformation of the volcanic cone by regional strike slip displacements, height of the volcanic cone, and position of the sample in the volcanic system (central or lateral) are included. Note the position of the Bullerengue-1 gas condensate well producer level in the Lower Magdalena Basin (VIM). Note that the mud volcanoes in the Sinú Fault Footwall Realm (Sinú basin area - Sn) mainly detach from Oligocene to Miocene stratigraphic levels, in the San Jacinto Footwall Realm from Early Paleocene - Eocene and some volcanoes from Neogene stratigraphic levels (Serranía de Tubará - Sr.T. and Serranía del Sinú - Sr. S.) and along the San Jacinto Hangingwall Realm from Cretaceous and Oligocene stratigraphic levels (Lower Magdalena Basin - VIM and Serranía de San Jacinto - Sr.S.J.)

values lower than 0.4, such as those observed in mud volcanoes of Family one and part of Family Two (Figure 5), are characteristic of sediments from metalliferous sedimentary sources or from volcanic arcs with significant basaltic input. Furthermore, the remaining mud volcanoes of Family two (Serranía de Tubará and VIM basin), with values higher than 0.4, would indicate sedimentary origins from sources rich in terrigenous sediments or volcanic arcs formed in subduction margins with high sedimentary contribution (Figures 4 and 5). Therefore, it can be argued that Family One mud volcanoes cut and drag sediments from formations whose source areas were composed of basaltic rocks (such as outcrops along the Western Cordillera), whereas Family Two mud volcanoes cut and drag sediments from formations whose source areas were composed by granitic - magmatic volcanic arcs rocks (like the outcrops in the Santander massifs and Central Cordillera).

U/Pb AGES IN ZIRCONS AS INDICATOR OF PROVENANCE OF SEDIMENTARY SEQUENCE'S CROSSED BY MUD VOLCANOES

U/Pb ages obtained from detrital zircon crystals recovered from the mud volcanoes analyzed for this work (youngest zircon grain, youngest population age, four youngest populations of ages, and four oldest age populations), suggest that the sedimentary sequences crossed by the mud volcanoes of Family one and part of Family two (southern Serranía de San Jacinto) had sedimentary input

from the Upper Miocene - Pleistocene, Lower Miocene, Eocene, and Cretaceous igneous or metamorphic massifs (Figures 6 and 8). The same approach for family two of the mud volcanoes (northern Serranía de San Jacinto, Serranía de Tubará, and VIM basin) suggests that the sedimentary sequences crossed by the mud volcanoes had Paleocene-Cretaceous, Triassic-Jurassic, lower Paleozoic and Neoproterozoic sedimentary input from igneous or metamorphic massifs (Figures. 6 and 8).

The zircon ages obtained in the San José de Mulatos mud volcano (74 Ma single peak), seem to correspond to a particular zircon enrichment event. Samples from lower to middle Miocene outcrops of the Campano, Pavo, and Floresanto formations, near to the Urabá Gulf (around the mud volcano), persistently show large zircon content (more than 40 grains), with preferential ages between 74 to 78 Ma (Figure 7). Thus, it can be considered that the San José de Mulatos mud volcano crosses predominantly Miocene stratigraphic sequences, which received sedimentary input from igneous or metamorphic sources of Cretaceous age (Figure 7).

PROPOSED REGIONAL REALMS OF NORTHERN COLOMBIA MUD VOLCANOES.

Few works use micropaleontological or palynological recovery to define the possible levels of detachment of mud volcanoes in Colombia (Trejos-Tamayo *et al*., 2020), and those that include detrital zircon ages are not available. Rather, more works concentrate on geochemical analyses of mud and fluids in an attempt to explain the genesis of the phenomenon (Carvajal and Mendivelso, 2017; Dill and Kaufhold, 2018; di Luccio *et al*., 2021). Nonetheless, mud volcanoes can take off several kilometers deep, being considered as windows through which samples of the traversed rocks emerge (Sautkin *et al*., 2003). Thus, the results of the U/Pb ages in detrital zircons, the recovery of faunas (micropaleontology and palynology), and the geochemical characterization of the samples analyzed in this work suggest the age and composition of the formations from those that detached or were crossed by the mud that formed the volcanoes in the Caribbean of Colombia. Thus, it is possible to establish three large domains of mud volcanism, bounded by regional thrust faults in northern Colombia, such as Sinú and San Jacinto (Figure 9). According to their structural position with respect to these large faults, the proposed domains of the mud volcanoes are: a) Footwall realm of the Sinú Fault; b) Footwall realm of the San Jacinto Fault; c) Hangingwall realm of the San Jacinto Fault.

Sinu Fault Footwall Realm:
This realm is located to the west of the Sinú Fault (which includes the southern extension of the Sinú basin), composed of mud volcanoes such as Virgen del Cobre, which, according to the U/Pb age of the detrital zircons recovered in this work, detached from Oligocene sedimentary sequences, to mud volcanoes such as Arboletes, which seem to be detached from Lower Miocene to Quaternary sedimentary sequences (Figures 13 and 14). The ages of the recovered foraminiferal faunas (planktonic and benthic), nannofossils and palynology support these detachment ages (early to middle Miocene), except for the Cretaceous nannofossil recovery from the Virgen del Cobre volcano (Table 3 and Figure 10). Considering that the U/Pb age of the zircons recovered in this volcano, as well as that of the detrital zircons of the outcropping formations, is predominantly Cretaceous (Figure 7), it is possible to consider that the recovered nannofossils are the reflection of reworked sediments of this age, accumulated in Oligocene – Miocene sequences and expelled by the mud volcano currently. These ages are consistent with published studies, which suggest a good correlation between biostratigraphic ages from samples of the Arboletes volcano, and the lower Miocene bedrock (Trejos-Tamayo *et al*., 2020).

San Jacinto Fault Footwall Realm:
The area bounded between the Sinú and San Jacinto faults define this realm, involving the Serranía del Sinú, the Serranía de San Jacinto, and the Serranía de Tubará. The U/Pb ages obtained from detrital zircons (Figures 6 to 9), jointly with the oldest ages obtained from pollen, planktonic-benthic foraminifera, and calcareous nanofossils recovery (Table 3 and Figure 10), suggest four main levels of detachment for the mud volcanoes studied in this realm:

a) Paleocene - Eocene detachment level, of mud volcanoes such as El Tesoro, Cañaveral, and Las Palomas (Figure 13), of which the El Tesoro volcano, despite being born in Neogene sedimentary sequences, crosses Paleocene-Eocene rocks in the hangingwall of a regional thrust (Figure 14). The relationships between the biostratigraphic ages of the mudstones of El Tesoro mud volcano (San Antero) and the bed rock also suggest an Eocene age for the detachment level (Trejos-Tamayo *et al*., 2020).

b) Middle to upper Eocene detachment level of mud volcanoes such as El Rodeo, El Reposo, and El Olivo (Figure 13), based mainly on the oldest ages obtained from calcareous nanofossils. Only the El Rodeo volcano (central and lateral craters) shows U/Pb ages in detrital zircons related to middle to upper Eocene sedimentary sequences, while the El Reposo and El Olivo volcanoes show detrital zircons with U/Pb ages related to Miocene sedimentary sequences (Figures 9, 10 and 13). It is interesting to note that the El Olivo volcano is located less than 2 km away from the Las Palomas volcano, whose level of detachment is interpreted to be from the middle Paleocene to lower Eocene (Figure 13), suggesting that despite their proximity, the mud volcanoes can come from different detachment levels, either due to the existence of multiple overpressure levels in the same sector, or due to shale allokinesis. This is also true in the El Reposo - Yerbabuena mud volcanoes area, which separation is less than 5 km, where seismic data suggest a basal level of mid-Eocene detachment for the former, which migrates towards the west, up to Oligocene detachment levels for the second (Figures 13 and 14). In this context, it is likely that the micropaleontological, palynological, and detrital ages of the zircons reflect the allokinetic processes of the shales as generators of some mud volcanoes of the Serranía de San Jacinto and Serranía de Tubará.

c) A probable Oligocene detachment level of mud volcanoes such as La Laguna, Santa Catalina, and Yerbabuena, can be inferred from comparisons of U/Pb ages in detrital zircons from their shales with zircons recovered from host rocks, as well as contributions from Lower Miocene sequences, according to micropaleontological studies and palynological ages (Figure 13). As previously mentioned, the Yerbabuena mud volcano seems to be the expression of a local shale allokinetic process related to the El Reposo volcano, while the Santa Catalina and La Laguna volcanoes, according to the morphostructural analysis, suggest that the dextral movement of regional faults such as Clemencia and San Jacinto, respectively (Figures 1 and 2), can control the expulsion of shales from Oligocene levels.

d) The youngest stratigraphic level of mud volcano detachment in this area is of Miocene age, from which the mud volcanoes El Totumo, Flamenco, Puerto Escondido, and San José de Mulatos apparently originate (Figure 13). Clay mineralogy analysis suggests that volcanoes such as El Totumo and Flamenco eject mud from sequences buried less than 1 km away, while Puerto Escondido and San José de Mulatos come from deeper sedimentary sequences, whose predominant age is the Miocene. This interpretation is consistent with the expression that these volcanoes have in adjacent seismic lines (Figure 14), as well as the biostratigraphic ages from

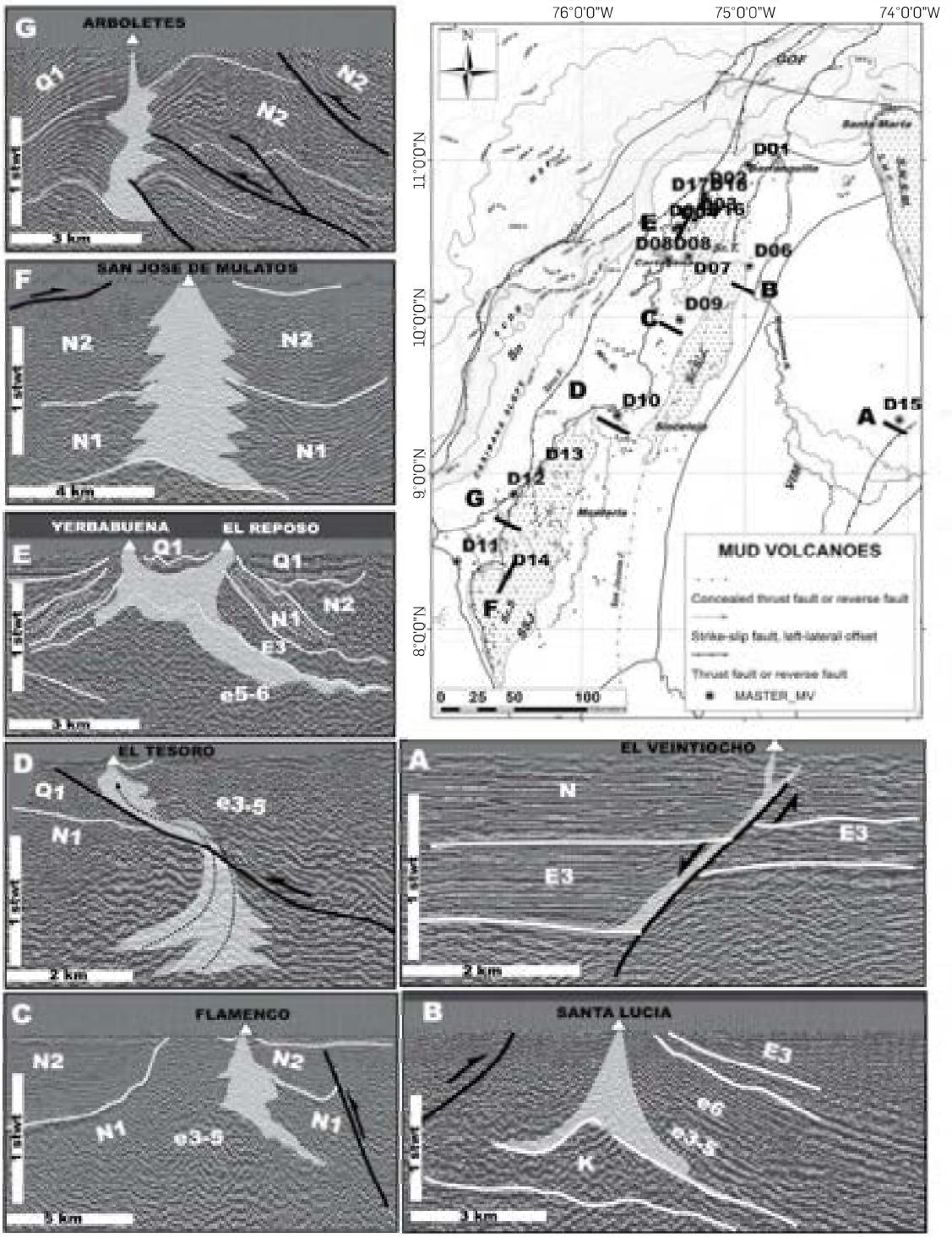

Figure 14. Distribution map of mud volcanoes and seismic expression of some of the volcanoes studied in this work. Seismic lines were acquired during the O&G exploration activities conducted by the ANH and private exploration companies in northern Colombia during the last 4 decades. Note that mud volcanoes in the San Jacinto Hangingwall Realm, suggest a clear relation with faults that affect the basement of the Lower Magdalena Basin (Seismic line A) or above Late Cretaceous - Paleogene sedimentary sequences affected by overpressure processes (Seismic line B). In the San Jacinto Footwall Realm, the seismic lines reveal that mud volcanoes occur near thrust faults (Seismic line C), cross a thrust fault plane (Seismic line D), suggest and alloquinetic movement of the mud (Seismic line E), or vertical movement from deeper levels (Seismic line F). The Arboletes mud volcano (and probably the Virgen del Cobre mud volcano) reflect the interaction between the San Jacinto and Sinu Footwall Realms, developed near large thrust fault planes affecting mainly Miocene to Quaternary sedimentary sequences (Seismic line G).

samples from the Puerto Escondido volcano (Trejos-Tamayo *et al.*, 2020) and XRD analysis of clays from the El Totumo mud volcano (Dill and Kaufhold, 2018).

San Jacinto Fault Hangingwall Realm:
Only two volcanoes in this sector were analyzed, Santa Lucía, and El Veintiocho (the most continental mud diapiric expression recorded in northern Colombia), both circular, expelling clasts and splashes. Of these volcanoes, Santa Lucía appears to be detached from the Paleocene-Eocene age sequences, according to the U/Pb age of the youngest zircon grain, as well as the age of planktonic foraminifera and calcareous nannofossils (Figure 10). The El Veintiocho mud volcano, on the other hand, appears to be detached from Oligocene sequences, according to the oldest pollen record analyzed and the U/Pb age of the youngest zircon grain (Figures 9, 10 and 13). Seismic reflection profiles show that the El Veintiocho mud volcanism occurs in a less than 1.5 km sedimentary thicknesses (Figure 14), over traces of normal faults affecting a basement considered of continental affinity (Cediel, et al., 2005), covered by sedimentary sequences with ages from Oligocene to Quaternary (J. Mora *et al.*, 2018), consistent with the ages recorded in the circon grains analyzed by U/Pb method, and palynological recovery obtained from the mud volcano samples. To the north, seismic information, combined with geological cartography and regional basin studies (Mora *et al.*, 2018), suggest that the Santa Lucía mud volcano detach from the middle Paleocene to the lower Eocene stratigraphic sequences, without ruling out contributions from Cretaceous sedimentary sequences (Figure 14). This is consistent with U/Pb ages of detrital zircons, as well as with micropaleontological and palynological recoveries obtained from mud volcano samples (Figures 9, 10 and 13). It is worth mentioning that on the western flank of the Santa Lucia mud volcano, there are isolated carbonate blocks, over 3 m in diameter, surrounded by very sheared mudstones, suggesting their expulsion from the subsurface. Micropaleontological ages obtained from these blocks suggest a middle Eocene age, as well as the presence of algal rhodoliths, which are common in Eocene formations such as the Maco. Fluid analysis in the shale deformed by the Santa Lucía mud volcano shows high organic matter content, very similar to those observed in several Cretaceous localities in the Colombian Caribbean (Gonzalez-Penagos, 2019).

FLUIDS AND GASES

The origin of the waters expelled by mud volcanoes is not easy to identify, as their ascent occurs through conduit systems, which pass through various geological formations with different formation waters. Isotopic analyses of waters recovered from mud volcanoes (Mazzini and Etiope, 2017), suggest three origins: a) fresh/marine water trapped mechanically during rapid burial periods; b) waters expelled during diagenesis of clay minerals (perhaps the most important source of water in mud volcanoes); c) shallow meteoric waters (isotopically trending towards the global meteoric water baseline). The $\delta^{18}O$ vs δD ratio for the mud volcano samples analyzed in this study show a clear negative linear trend, with values that are characteristic of formation waters (Figure 11 and Table 5). Comparison with isotopic results obtained in other mud volcanoes around the world allows us to pose scenarios about the formation processes of the waters in these structures.

Comparative analysis of $\delta^{18}O$ vs δD isotope ratios obtained in mud volcanoes from the southern Caspian Basin, Java, Italy, West Indies and Colombian Caribbean (Figure 11 and Table 5), suggest diagenetic origins from clay minerals at depths greater than 3 km (Martinelli and Judd, 2004; Madonia et al., 2011; Agustawijaya et al., 2017; Mazzini and Etiope, 2017; di Luccio et al., 2021); however, volcanoes in the Caspian area, usually have much lower δD values (between -20 ‰ and -60‰) and does not have a negative linear relationship as it occurs in the other mud volcanoes (Figure 11 and Table 5). Unlike the mud volcanoes of Java, Italy, and the West Indies, the Caspian mud volcanoes are subjected to a high sedimentation rate of about 2.4 km/Ma, burying Oligo-Miocene sequences to depths of more than 10 km. This extreme burial may result in high diagenetic conditions on clay sequences, and allow the expulsion of diagenetic waters with higher isotopic differentiation. In the case of the Caribbean mud volcanoes of Colombia, it is observed that they coincide, in general, with the regional trend of the West Indies, as well as with the Lusi volcano in Java, except for the La Laguna and Virgen del Cobre mud volcanoes, which have a marked tendency to approach the global meteoric water line (Figure 11 and Table 5). It is likely that their proximity to regional faults on the coastline allows infiltration of meteoric water and seawater wedge, affecting the original hydrogeochemical signal.

It is striking that the volcanoes studied in the Colombian Caribbean seem to separate into two families (trends 1 and 2), one of which tends to be below the isotopic trend marked by the Antillean volcanoes and the other above (Figure 11 and Table 5). Comparing these families with the previously proposed detachment levels for the Colombian Caribbean, it is observed that volcanoes with $\delta^{18}O$ vs δD ratios, above the regional trend for West Indian volcanoes, match volcanoes with stratigraphic detachment from Neogene-Quaternary sedimentary sequences, except for the Yerbabuena, Tesoro and Olivo volcanoes, while volcanoes with $\delta^{18}O$ vs δD ratios below this trend probably have detachment levels from Paleogene sequences (Figures 11 y 13). The Yerbabuena volcano shows $\delta^{18}O$ vs δD isotope ratios above the regional trend for West Indian volcanoes (Figure 11 and Table 5); however, it shows evidence of mud from Oligocene sequences. This volcano is less than 5 km from the mud volcano El Reposo, which shows evidence of muds from the Eocene and its $\delta^{18}O$ vs δD isotopic ratio is below the West Indian trend line (Figures 11 and 13). Seismic information shows that both volcanoes may be connected (Figure 14), suggesting two levels of hydric enrichment, one Paleogene (which would feed El Reposo volcano), and the other Neogene (which would feed Yerbabuena volcano), with contributions of mud from older (Eocene - Oligocene) detachment levels.

El Tesoro volcano presents the highest $\delta^{18}O$ values, very similar to those reported in Java and Italy (Figure 11 and Table 5); however, it evidences mud transporting from Paleocene - Eocene sequences. Previously, it was observed that this volcano is in the hangingwall of a reverse fault - very close to the trace - in contact with Paleocene-Eocene sequences over Neogene sequences (Figure 14). Thus, it can be considered that the El Tesoro mud volcano transports materials from Paleocene-Eocene sequences of the hangingwall, thanks to the injection of fluids from the Miocene sequences in the underlying block. In this scenario, the isotopic composition of the analyzed waters would not represent the fluids of the hangingwall (Paleogene sequences), representing the waters expelled from the foot wall (Neogene sequences). El Olivo volcano is similar to El Tesoro volcano, with isotopic signatures of water expelled from Neogene stratigraphic sequences, but with evidence of Eocene detachment (Figure 13). There is no evidence of faults that would allow enriching the volcano mud with fluids from Oligo-Miocene sequences. However, less than 2 km away is the El Totumo volcano, which detaches from Miocene sedimentary sequences (Figure 13), suggesting the presence of 2 nearby detachment levels, which enrich muds from older sequences (Eocene) with fluids from younger sequences (Miocene), with $\delta^{18}O$ vs δD isotope ratios above the regional trend of mud volcanoes in the Antilles.

Despite the low Cl- contents obtained in this study (between 2000 and 8000 mg/l), compared to the values from previous works in

the area (di Luccio *et al.*, 2021), their correlation with the difference between the $\delta^{18}O$ value and the local meteoric water line, allows discriminating the families defined above (Figure 11 and Table 5). This suggests that trend 1 presents higher initial Cl- contents before the diagenesis (>12000 mg/l)starts, while trend 2 presents lower Cl- content (< 9000 mg/l). This anionic-isotopic relationship seems to confirm the presence of two levels of diagenetic water expulsion, at different stages of thermal maturity, evidenced by different volumes of expelled water. Some volcanoes do not respond to these trends, such as Santa Catalina (Paleogene detachment and initial Cl- contents <9000 mg/l) and Virgen del Cobre (Paleogene detachment with initial Cl- contents >12000), which are very close to regional faults such as Clemencia and Uramita respectively. It is possible that faults such as Clemencia, allow the expulsion of mud from Paleogene sequences, enriched with diagenetic waters of the Neogene, less rich in Cl-.

The Virgen del Cobre volcano is a particular case, because the sedimentation in the Serranía del Sinú and Sinú occurs during the last 20 Ma (López, 2019; López-Ramos *et al.*, 2021), making impossible the contribution of trend 2 of fluids from Paleocene or Eocene sedimentary sequences. However, this volcano is located 10 km from the Uramita Fault, the tectonic boundary between the Panama block and the South American northwest (Vargas, et al., 2005; Wagner *et al.*, 2017), with dips exceeding 3 km and decollement at more than 7 km depth, involving basement of oceanic nature (Flinch, 2003; Garzón, 2012). Considering the regional character of the Uramita Fault, it is possible to consider that fluids resulting from the transformation of clay minerals along the decollement allow the expulsion of poorly chlorinated waters and little isotopic dephasing. The low Cl- contents obtained in this study compared to previous studies (di Luccio *et al.*, 2021), may be related to factors such as sampling site (tap, crater, pool), prevailing meteorological conditions (prolonged summer periods vs. winter seasons) and water preservation processes (Mazzini and Etiope, 2017).

The molecular and isotopic compositional analyses of the methane recovered in the mud volcanoes appear to come from petroleum systems at various degrees of maturity, as deduced from the results obtained in the CO_2 analyses, suggesting that each mud volcano is a surface manifestation of a petroleum system in the subsurface (Figure 12 and Table 6). Thus, when observing the spatial distribution of the mud volcanoes grouped according to CO_2 origin, there is a clear tendency to present evidence of hydrocarbons associated with late mature petroleum systems along the Serranía de San Jacinto, while along Serranía del Sinú, there are petroleum systems that vary between biogenic and early thermogenic (Figure 12 and Table 6). Lastly, in the Sinu basin area, data are only presented in the Virgen del Cobre mud volcano, which indicates a tendency to gases associated with petroleum systems in a window of early oil generation (Figure 12 and Table 6). At some points in the Sinú Basin, sediment samples have been recovered in submarine chimneys, by piston core, with gases of thermogenic origin, very close to the trace of frontal faults of the South Caribbean deformed belt (Sanabria and Ramirez, 2018). In some convergent margins, the presence of gases and fluids of thermogenic origin have been reported along regional faults, with deep detachments, associated with the progressive increase in temperature and pressure undergone by sediments when entering the regional detachment zones at more than 10 km depth (Lutz *et al.*, 2004; López-Ramos, 2016). Thus, it can be considered that the gases emanated by the Virgen del Cobre volcano may be the expression of thermogenic petroleum systems developed along deep detachments of regional faults such as the Uramita Fault. Although there are no gas or fluid samples, El Olivo and Santa Lucia volcanoes show evidence of hydrocarbons in blocks expelled through the craters (Figure 12 and Table 6). The origin of hydrogen in the gases analyzed is still to be studied , since the proximity to regional faults and basements of oceanic nature provide optimal conditions for migration of abiogenic hydrogen to the surface.

CONTROLLING MECHANISM OF MUD VOLCANISM IN THE COLOMBIAN CARIBBEAN

There is evidence of mud volcanoes in the maritime and continental domains of northern Colombia (Figure 1). Seismic reflection profiles and bathymetric information, as well as satellite images and high-resolution digital global elevation models, allow us to define the location and basic morphological characteristics such as area, ellipticity, and height of the volcanoes (Table 1). The integration of the mud volcano data allowed us to distinguish 4 blocks with different morphological characteristics. It is observed that in the marine domain, the most frontal and central part of the Sinu basin has the lowest quantity of mud volcanoes per cell of 25 km^2

Table 6. Data of isotopic δ13C1 vs δ13CO2 in gas samples recovered from Colombian Caribbean mud volcanoes for this work (see Fig. 12 for graphic relationships). The mud volcanoes column refers to the number of the analized mud volcano (Names of mud volcanoes in Tables 2 and 3 and location in Fig. 1).

Sample	H_2	O_2+ Ar	CO_2	N_2	CO	C_1	C_2	C_2H_4	C_3	C_3H_6	iC_4	nC_4	iC_5	nC_5	C_6+	$\delta^{13}C_1$	$\delta^{13}C_2$	$\delta^{1}DC_1$	$\delta^{13}CO_2$
Name	ppm	ppm	ppm	ppm	ppm	ppm	ppm	ppm	ppm	ppm	ppm	ppm	ppm	ppm	ppm	‰	‰	‰	‰
D-09	nd	233000	640	639600	nd	126600	nd	147	nd	nd	nd	nd	1	nd	18	-38,0		-142	-8,1
D-01	nd	237200	1200	918700	nd	142700	17	178	nd	nd	nd	nd	nd	nd	21	-52,6		-185	-9,0
D-02	nd	217300	500	751400	nd	30800	nd	30	nd	nd	nd	nd	nd	nd	11	-62,0		-204	-12,1
D-03	nd	70000	7000	222600	nd	699700	572	nd	95	nd	23	6	3	nd	38	-58,3	-53,4	-211	3,5
D-04	nd	208400	700	760800	nd	30100	nd	14	nd	nd	nd	nd	nd	nd	12	-61,0		-185	-10,5
D-05	nd	127800	1900	434000	nd	436000	256	nd	6	nd	nd	nd	nd	nd	33	-65,5	-36,0	-194	-14,9
D-07	nd	179700	1700	653400	nd	165000	187	nd	13	nd	nd	nd	nd	nd	19	-48,5		-182	13
D-078	nd	201300	510	729600	nd	68600	nd	9	nd	nd	nd	nd	nd	nd	13	-47,9		-182	-5,1
D-08	nd	215100	440	778200	nd	6280	nd	20	nd	nd	nd	nd	nd	nd	7	-59,1		-189	
D-088	nd	154500	1900	561800	nd	281800	nd	nd	nd	nd	nd	nd	nd	nd	21	-61,5		-193	-6,2
D-13	nd	22200	17500	65600	nd	894600	106	nd	11	nd	nd	nd	nd	nd	nd	-55,6		-190	10,3
D-11	nd	177600	2800	629100	nd	190400	57	nd	5	nd	nd	nd	nd	2	2	-56,8		-184	-14,1

(the boundary between blocks 1 and 2), as well as the Magdalena Submarine Fan and the southern part of the Guajira Offshore basin (Figure 1).

The Magdalena Submarine Fan zone is affected by some faults and is characterised by the greatest sedimentary thicknesses in the Colombian Caribbean, exceeding 5 km of sediments accumulated during the last 5 Ma (López, 2019; López-Ramos *et al.*, 2021). One of the mechanisms that form mud volcanoes is the overpressure produced in thick, rapidly deposited sedimentary sequences, especially muddy ones (Kopf, 2002; Jiang *et al.*, 2011; Kassi *et al.*, 2014); however, along the Magdalena Submarine Fan, the presence of mud volcanoes is not noticeable. It is likely that the large presence of mud, coupled with the rapid advance of the Magdalena Submarine Fan over the Caribbean Basin, avoid the generation of weak zones through which fluids migrate to the surface, preventing the formation of mud volcanoes. The central zone of the Sinú basin is characterized by thicknesses smaller than those recorded in the Magdalena Submarine Fan, accumulated over a longer period of time, affected by complex thrust systems, with a regional detachment that can exceed 8 km depth under the South American margin (Corredor, et al., 2003; Flinch and Castillo, 2015; Rodríguez, 2020).

Compressional zones with geometry and lithology similar to that of the Sinú basin have been studied in the Canadian Pacific margin, the eastern Mediterranean, and Barbados, suggesting that in this type of prism, areas with a predominantly compressive component develop, where there is an equilibrium between lithostatic and fluid pressure along the decollement, decreasing the formation of mud volcanoes or the leak of fluids to the surface in these zones (Tobin *et al.*, 1993). As the compressional component decreases, and the strike-slip component increases, the lithostatic vs. fluid equilibrium is lost, especially by the formation of transfer faults, or by their contact with the basement backstop, allowing fluids to leak to the surface (Tobin *et al.*, 1993; Camerlenghi *et al.*, 1995; Chamot-Rooke, et al., 2005). Thus, blocks 1 and 2 (south of the Magdalena Submarine Fan and the entire Sinú basin and Serranía del Sinú), may be the expression of the contact between the deformed sedimentary prism (***Sinu Fault Footwall Realm***) and the rigid backstop (***San Jacinto Footwall and Hangingwall Realm***), as well as the transition from net compression zones to stress partitioning (blocks 2 and 3), relieving overpressures in regional detachment zones. In such conditions, a large number of volcanoes/25km^2 may occur outside the areas of net compression, with mud volcanoes whose areas tend to be small (little expulsion of material to the surface), variable ellipticity, controlled by their proximity to faults with strike-slip components, and relatively high volcanic edifices (Table 1). Block 3, with a high number of mud volcanoes/25km^2, located mainly in the ***San Jacinto Hangingwall Realm***, is affected by important strike-slip faults such as Oca, with important values of ellipticity and heights of the volcanic edifices, similar to those observed in Block 2 (Table 1), confirming that the increase in ellipticity of the mud volcanoes is linked to the increase of the strike-slip component in regional faults. A topic to be developed in further studies is the relationship between mud volcano activity and the occurrence of seismic events in the Caribbean, especially in block 1 of mud volcanoes, due to its proximity to the collision zone of the Panama Arc against the NW corner of South America.

The central zone of the Guajira Offshore basin is characterized by thick sedimentary sequences accumulated during the Miocene - Pliocene, over the rigid backstop zone (***San Jacinto Hangingwall Realm***), trapped in intraslope basins (Ramirez *et al.*, 2015). It is possible that being retained in an area of the rigid backstop, faults that allow the escape of fluids, or the formation of compressive structures, are not present. Block 4 of mud volcanoes (***San Jacinto Hangingwall Realm***), located in the northern part of the Guajira Offshore basin, presents the smallest area of exposure (greater volume of expelled mud), with an intermediate number of volcanoes/25km^2, a higher average area than all those analyzed in other blocks, little ellipticity and relatively low (Table 1). Most of these volcanoes are formed on regional gravity gliding zones, along which, through normal faults in the extensional domain or reverse faults in the compressional domain, allow the outflow of fluids to the surface, developing chimney and diapir systems (W. Martinez *et al.*, 2016). In margins such as Nigeria, where large gravity gliding develops seismic information suggests that in the transition between the translational domain of the block to the compressive domain of the slide, the seismic reflection interval velocities tend to form an upward ramp that when passing the detachment level of the slide, decreases again, indicating that there is a zone of overpressure in the compressive part of the gravity slide (Albertz, et al, 2010). Thus, a mechanism that may be controlling the formation and distribution of mud volcanoes in the offshore of the upper Guajira may be linked to the development of gravitational landslides.

OIL POTENTIAL

Areas with mud volcanoes were particularly attractive for hydrocarbon exploration, resulting in abundant oil and gas production in the South Caspian Basin, but prematurely abandoned worldwide, due to difficulties in drilling areas with overpressured shales, with abundant gas in the system, and reservoirs dispersed in thick mud sequences (Hedberg, 1974). The comprehensive analysis of mud volcanoes allows us to propose mechanisms that have controlled them in the maritime and continental domains of northern Colombia. Thanks to the identification of these mechanisms, as well as the possible rocks from which they take off, and the sedimentary sequences they cross, added to the geochemical results of extracted fluids and gases, it is likely that thermogenic petroleum systems may be present in the area, hidden or affected by the overpressure conditions that generate mud volcanism. Mud volcanoes such as Santa Lucia show in the transported blocks, hydrocarbons of thermogenic origin, as well as the hosted rock expelled to the surface by the overpressure. This mud volcano occurs just south of the Perdices and Bullerengue hydrocarbon fields, composed of condensate oil and rich gas (Figure 13), which are characterized by overpressure zones in Mio-Oligocene units. It is possible to deduce, based on the bio and geochronological recoveries obtained in the muds and carbonate blocks of the Santa Lucía volcano, that Paleogene (Eocene) sedimentary sequences, close to Miocene - Oligocene overpressure zones, were detached and brought to the surface, forming the mud volcanic system. Blocks transported by the mud to the surface have evidence of liquid hydrocarbons, as well as mud extracts, with geochemical signatures similar to the Cretaceous of the Cansona Fm. (Gonzalez-Penagos, 2019). These evidences allow us to state that the mud volcanics in the VIM and Serranía de San Jacinto (***San Jacinto Hangingwall and Footwall Realms***), present evidence of petroleum systems associated with liquid thermogenic hydrocarbons, produced from Cretaceous rocks and stored in siliciclastic and calcareous Paleocene and Eocene reservoirs. Zones adjacent to large faults in Serranía del Sinú, show gases and liquid hydrocarbons of thermogenic origin, probably associated with leaks through volcanic mud systems, of fluids generated at great depths, or through faults, allowing the partial filling of Miocene and Pliocene reservoirs as revealed by exploratory wells such as Cordoba-1 (***Sinú Footwall Realm***). Zones with thinner

thicknesses in the Sinú basin area tend to preserve gases of biogenic origin, as reported by numerous exploratory wells such as Kronos-1, Glaucus-1, Fuerte-1 and Uvero-1 (Sinú Footwall Realm).

6. CONCLUSIONS

The regional diapir analysis shows the extent of the mud volcanic phenomenon in northern Colombia. The field study, with the acquisition of information of varying resolutions, allowed observing variations in terms of morphology and recent deformational processes, distinctive among volcanoes formed in different structural domains. Thus, volcanoes formed in the Lower Magdalena Basin are generally circular, connected to basement faults or regional thrusts, while volcanoes formed in the Serranía de San Jacinto and Sinú basins tend to present ellipsoidal shapes, with gully and drainage patterns that suggest the development of local stress fields associated with dextrolateral movements of major faults.

The clay minerals and geochemical analyses indicate that the volcanoes located in the Lower Magdalena Basin and the northern part of Serranía de San Jacinto contains mudstones that originated in sedimentary sequences with contributions from highly evolved continental basement, while the volcanoes in the central and the southern part of the studied area tend to show signs of sedimentary sources rich in minerals from magmatically less evolved areas. The U/Pb age relationships of zircons, micropaleontology and pollen suggest that the mud volcanoes have different levels of stratigraphic detachment: (a) from Paleocene - Eocene sequences, the Santa Lucia, Las Palomas, Cañaveral, and El Tesoro mud volcanoes; (b) from middle to upper Eocene sequences, the El Olivo, El Reposo, and El Rodeo mud volcanoes; c) from Oligocene sequences, the mud volcanoes El Veintiocho, La Laguna, Santa Catalina, Yerbabuena, and Virgen del Cobre; d) from Neogene sequences, the mud volcanoes El Totumo, Flamenco, Puerto Escondido, Mulatos, and Arboletes. These proposed levels coincide with the results obtained in the isotopic analysis of water recovered from the gryphons of mud volcanoes and their anionic content. However, volcanoes such as Virgen del Cobre, Santa Catalina, El Tesoro and El Olivo, present processes of enrichment of somewhat chlorinated waters, because of their proximity to regional faults or shallower detachment levels.

The distribution and morphological characteristics of mud volcanoes in the Caribbean suggest various processes that form overpressure zones and mud volcanism. Much of the Southern Caribbean Deformed Belt is controlled by stress partitioning between the Caribbean and South American plates, as well as an increase in the strike-slip component of major faults, while in the northern part of the Guajira Offshore basin, mud volcanism appears to be controlled by the development of regional gravity instabilities. Volcanism in the Lower Magdalena Basin appears to be linked to fault traces affecting the basement of the area.

Gas and water analyses suggest that the older Paleocene belts and the rigid backstop area have evidence of fluids and gases from predominantly thermogenic petroleum systems, while in the younger deformed belt domain, the tendency is to have microbial petroleum systems.

ACKNOWLEDGEMENTS

This work has been the result of joint research projects between the Vice-Presidency of Exploration of Ecopetrol and the Colombian Petroleum Institute. We thank both entities for their support to the execution of these projects, as well as the project leaders and laboratories that participated in them.

REFERENCES

[1] Aguilera, R., Cediel, F., Ojeda, G. Y., & Colmenares, F. (2011). Geology and hydrocarbon potential Sinú and San Jacinto basins. *Petroleum geology of Colombia*, 12. http://www.scielo.org.co/pdf/boge/v44n1/2145-8553-boge-44-01-15.pdf

[2] Agustawijaya, D. S., Karyadi, K., Krisnayanti, B. D., & Sutanto, S. (2017). Rare earth element contents of the Lusi mud: An attempt to identify the environmental origin of the hot mudflow in East Java–Indonesia. *Open Geosciences*, 9(1), 689-706. https://doi.org/10.1515/geo-2017-0052.

[3] Albertz, M., Beaumont, C., & Ings, S. J. (2010). Geodynamic modeling of sedimentation-induced overpressure, gravitational spreading, and deformation of passive margin mobile shale basins. https://doi.org/10.1306/13231307M933417.

[4] Amajor, L. C. (1987). Major and trace element geochemistry of Albian and Turonian shales from the Southern Benue trough, Nigeria. *Journal of African Earth Sciences* (1983), 6(5), 633-641. https://doi.org/10.1016/0899-5362(87)90002-9.

[5] ANH (2005). Sinu – San Jacinto Basin. Bogotá DC: *Agencia nacional de Hidrocarburos*. https://www.anh.gov.co/documents/4205/Sin%C3%BA_San_Jacinto_PDF.pdf

[6] ANH, C. S. B. (2007). Nomenclature, boundaries and petroleum geology, a New Proposal. Bogotá DC: *Agencia Nacional de Hidrocarburos*. https://catalogo.sgc.gov.co/cgi-bin/koha/opac-detail.pl?biblionumber=72947.

[7] Aristizábal, C., Ferrari, A., & Silva, C. (2009). Control neotectónico del diapirismo de lodo en la región de Cartagena, Colombia. *Ingeniería Investigación y Desarrollo:* I2+ D, 8(1), 42-50. https://dialnet.unirioja.es/descarga/articulo/6096122.pdf

[8] Baloglanov, E. E., & Mamedova, A. N. (2018). INTENSITY OF MUD VOLCANIC ACTIVITY–A HARBINGER OF EARTHQUAKE. *Theoretical & Applied Science*, (7), 148-153. https://doi.org/10.15863/tas.2018.07.63.23.

[9] Barrera, R. (2001). Geología de las Planchas 16-17 (Galerazamba y Barranquilla). *Ingeominas. Memoria Explicativa*, 3-54. http://recordcenter.sgc.gov.co/B4/13010010002331/documento/pdf/010102311101000.pdf.

[10] BARRERA, O. (2003). Geología de la plancha 43 San Antero-San Bernardo del Viento. *Ingeominas. Memoria Explicativa*. https://recordcenter.sgc.gov.co/B4/13010010002491/documento/pdf/010102491110100O.pdf.

[11] Triana, Y. D. B. (2018). *Sedimentary megasequences of Colombian basin, offshore Colombia* (Doctoral dissertation, The University of Arizona). https://repository.arizona.edu/handle/10150/631927.

[12] Bayona, G., Cardona, A., Jaramillo, C., Mora, A., Montes, C., Valencia, V., ... & Ibañez-Mejia, M. (2012). Early Paleogene magmatism in the northern Andes: Insights on the effects of Oceanic Plateau–continent convergence. *Earth and Planetary Science Letters*, 331, 97-111. https://doi.org/10.1016/j.epsl.2012.03.015.

[13] Bernal-Olaya, R., Mann, P., & Vargas, C. A. (2015). Earthquake, tomographic, seismic reflection, and gravity evidence for a shallowly dipping subduction zone beneath the Caribbean Margin of Northwestern Colombia. https://doi.org/10.1306/13531939m1083642.

[14] Bonini, M., Rudolph, M. L., & Manga, M. (2016). Long- and short-term triggering and modulation of mud volcano eruptions by earthquakes. *Tectonophysics*, 672, 190-211. https://doi.org/10.1016/j.tecto.2016.01.037.

[15] Bown, P. R., & Young, J. R. (1998). Calcareous nannofossil biostratigraphy. *British Micropaleontology Society Series, Chapman & Hall, London*, 16-28. https://doi.org/10.1007/978-94-011-4902-0_2

[16] Breen, N. A. (1989). Structural effect of Magdalena fan deposition on the northern Colombia convergent margin. *Geology,* 17(1), 34-37. https://doi.org/10.1130/0091-7613(1989)017<0034:SEOMFD>2.3.CO;2.

[17] Briceño, L. A., & Vernette, G. (1992). Manifestaciones del diapirismo arcilloso en el margen colombiano del Caribe. *Earth Sciences Research Journal,* (1), 21-30. https://www.academia.edu/3171088/Manifestaciones_del_diapirismo_arcilloso_en_el_margen_colombiano_del_Caribe.

[18] Bürgl, H. (1960). *Geología de la Península de la Guajira. Boletín Geológico,* 6(1-3), 129–168. https://doi.org/10.32685/0120-1425/bolgeol6.1-3.1958.314.

[19] Cadena, A. F., Romero, G., & Slatt, R. (2015). Application of stratigraphic grade concepts to understand basin-fill processes and deposits in an active margin setting, magdalena submarine fan and associated fold-and-thrust belts, Offshore Colombia. *Petroleum Geology and Potential of the Colombian Caribbean Margin.* 108, 323-344. https://doi.org/10.1306/13531942M1083646.

[20] Camerlenghi, A., Cita, M. B., Vedova, B. D., Fusi, N., Mirabile, L., & Pellis, G. (1995). Geophysical evidence of mud diapirism on the Mediterranean Ridge accretionary complex. *Marine Geophysical Researches,* 17, 115-141. https://doi.org/10.1007/BF01203423.

[21] Cardona, A., Valencia, V., Bayona, G., Jaramillo, C., Ojeda, G., & Ruiz, J. (2009). U/Pb LA-MC-ICP-MS Zircon Geochronology and Geochemistry from a Postcollisional Biotite Granite of the Baja Guajira Basin, Colombia: Implications for Late Cretaceous and Neogene Caribbean–South American Tectonics. *The Journal of Geology,* 117(6), 685-692. https://doi.org/10.1086/605776.

[22] Cardona, A., Valencia, V., Bustamante, C., García-Casco, A., Ojeda, G., Ruiz, J., ... & Weber, M. (2010). Tectonomagmatic setting and provenance of the Santa Marta Schists, northern Colombia: Insights on the growth and approach of Cretaceous Caribbean oceanic terranes to the South American continent. *Journal of South American Earth Sciences,* 29(4), 784-804. https://doi.org/10.1016/j.jsames.2009.08.012.

[23] Cardona, A., Valencia, V. A., Bayona, G., Duque, J., Ducea, M., Gehrels, G., ... & Ruiz, J. (2011). Early-subduction-related orogeny in the northern Andes: Turonian to Eocene magmatic and provenance record in the Santa Marta Massif and Rancheria Basin, northern Colombia. *Terra Nova,* 23(1), 26-34. https://doi.org/10.1111/j.1365-3121.2010.00979.x.

[24] Cardona, A., Valencia, V., Weber, M., Duque, J., Montes, C., Ojeda, G., ... & Villagomez, D. (2011). Transient Cenozoic tectonic stages in the southern margin of the Caribbean plate: U-Th/He thermochronological constraints from Eocene plutonic rocks in the Santa Marta massif and Serranía de Jarara, northern Colombia. *Geologica Acta,* 445-469. https://doi.org/10.1344/105.000001739.

[25] Cardona, A., Montes, C., Ayala, C., Bustamante, C., Hoyos, N., Montenegro, O., ... & Zapata, S. (2012). From arc-continent collision to continuous convergence, clues from Paleogene conglomerates along the southern Caribbean–South America plate boundary. *Tectonophysics,* 580, 58-87. https://doi.org/10.1016/j.tecto.2012.08.039.

[26] Cardona, A. (2014) *Basement geochronology from offshore and onshore Guajira basins:* R-11 and R12 blocks. (Documento interno). Instituto Colombiano del Petróleo. Bucaramanga, Colombia.

[27] Carvajal, J. H., & Mendivelso, D. (2017). Volcanismo de lodo del Caribe central colombiano. *Servicio Geológico Colombiano. Colección Publicaciones Especiales SGC.* https://doi.org/10.32685/9789585978201.

[28] Cediel, F., Shaw, R. P., & Cceres, C. (2003). Tectonic assembly of the northern Andean block *AAPG, The Circum-Gulf of Mexico and the Caribbean: Hydrocarbon Habitats, Basin Formation and Plate Tectonics,* (79), 815–848. https://doi.org/10.1306/M79877C37

[29] Ceramicola, S., Praeg, D., Cova, A., Loher, M., Bohrmann, G., & Mascle, J. (2020). Mud volcanoes and seafloor fluid seepage on the Calabrian accretionary prism (Ionian Sea). In *Memorie Descrittive Carta Geologica d'Italia* (Vol. 150, pp. 77-83). ISPRA, Servizio Geologico d'Italia. https://hal.science/hal-03551598/document.

[30] Ceron-Abril, J. F. (2008). *Crustal structure of the Colombian Caribbean Basin and margins* (Doctoral dissertation, University of South Carolina). https://www.proquest.com/openview/46eb3647887ab614994c0f91a80465b1/1?pq-origsite=gscholar&cbl=18750.

[31] Chamot-Rooke, N., Rabaute, A., & Kreemer, C. (2005). Western Mediterranean Ridge mud belt correlates with active shear strain at the prism-backstop geological contact. *Geology,* 33(11), 861-864. https://doi.org/10.1130/G21469.1.

[32] Chang, Z., Vervoort, J. D., McClelland, W. C., & Knaack, C. (2006). U-Pb dating of zircon by LA-ICP-MS. *Geochemistry, Geophysics, Geosystems,* 7(5). https://doi.org/10.1029/2005GC001100

[33] Chen, B., Liu, G., Wu, D., & Sun, R. (2016). Comparative study on geochemical characterization of the Carboniferousaluminous argillites from the Huainan Coal Basin, China. *Turkish Journal of Earth Sciences,* 25(3), 274-287. https://doi.org/10.3906/yer-1508-9.

[34] Clauer, N., & Chaudhuri, S. (2012). *Clays in crustal environments: isotope dating and tracing.* Springer Science & Business Media. https://doi.org/10.1007/978-3-642-79085-0.

[35] Clavijo, J., & Barrera, R. (2002) 'Geología de las Planchas 44 Sincelejo y 53 Sahagun', *Ingeominas. Memoria Explicativa* https://catalogo.sgc.gov.co/cgi-bin/koha/opac-detail.pl?biblionumber=14403

[36] Correa, I., Ríos, A., González, D., Toro, M., Ojeda, G., & Restrepo, I. (2007). Erosión litoral entre Arboletes y Punta San Bernardo, costa caribe colombiana. *Boletín de Geología,* 29(2), 115-129. https://www.redalyc.org/pdf/3496/349632018012.pdf.

[37] Corredor, F., Shaw, J., & Villamil, T. (2003, September). Complex imbricate systems in the southern Caribbean Basin, offshore northern Colombia: Advanced structural and stratigraphic analysis, and implications for regional oil exploration. In *8th Simposio Bolivariano-Exploracion Petrolera en las Cuencas Subandinas* (pp. cp-33). EAGE Publications BV. https://doi.org/10.3997/2214-4609-pdb.33.paper5.

[38] Deville, E., Battani, A., Griboulard, R., Guerlais, S., Herbin, J. P., Houzay, J. P., ... & Prinzhofer, A. (2003). The origin and processes of mud volcanism: new insights from Trinidad. *Geological Society, London, Special Publications,* 216(1), 475-490. https://doi.org/10.1144/GSL.SP.2003.216.01.31.

[39] Deville, E., Guerlais, S. H., Callec, Y., Griboulard, R., Huyghe, P., Lallemant, S., ... & Collaboration of the Caramba Working Group. (2006). Liquefied vs stratified sediment mobilization processes: insight from the South of the Barbados accretionary prism. *Tectonophysics,* 428(1-4), 33-47. https://doi.org/10.1016/j.tecto.2006.08.011.

[40] Dill, H. G., Ufer, K., Bornemann, A., Techmer, A., & Buzatu, A. (2019). From the strand plain to the reef: A sedimentological–geomorphological study of a Holocene coast affected by mud diapirism (Archipélago Rosario-Barú, Colombia). *Marine Geology,* 415, 105953. https://doi.org/10.1016/j.margeo.2019.05.012.

[41] DILL, H. G.; KAUFHOLD, S. The Totumo mud volcano and its near-shore marine sedimentological setting (North Colombia)—From sedimentary volcanism to epithermal mineralization. *Sedimentary Geology,* 2018, vol. 366, p. 14-31. https://doi.org/10.1016/j.sedgeo.2018.01.007.

[42] Domínguez, J. G., Gómez, J. C., Ricaurte, C., Mayo, G., Orejarena, J., Díaz, J. M., & Andrade, C. A. (2010). Cobertura de los fondos y paisajes bentónicos asociados a formaciones diapíricas en los Bancos de Salmedina, Plataforma Continental del Caribe Colombiano. *Boletín de Investigaciones Marinas y Costeras,* 39(1), 117–135. https://doi.org/10.25268/bimc.invemar.2010.39.1.145.

[43] Duque-Caro, H. (1979). Major Structural Elements and Evolution of Northwestern Colombia: Small Basin Margins. *Geological and geophysical investigations of continental margins: American Association of Petroleum Geologists Memoir 29.* https://www.scienceopen.com/document?vid=d9ce57fb-a2e0-45f8-834e-70a4194de21f.

[44] El-Wekeil, S. S., & Abou El-Anwar, E. A. (2013). Petrology, geochemistry and sedimentation history of Lower Carboniferous shales in Gebel Abu Durba, southwestern Sinai, Egypt. *Journal of Applied Sciences Research,* 9(8), 4781-4798. https://www.semanticscholar.org/paper/Petrology%2C-geochemistry-and-sedimentation-history-EL-Wekeil-El-Anwar/60fc11530756dd10921877f4d6378498a62b3fe6

[45] Fesharaki, O., GARCÍA-ROMERO, E., CUEVAS-GONZÁLEZ, J., & LÓPEZ-MARTÍNEZ, N. (2007). Clay mineral genesis and chemical evolution in the Miocene sediments of Somosaguas, Madrid Basin, Spain. *Clay minerals,* 42(2), 187-201.https://doi.org/10.1180/claymin.2007.042.2.05.

[46] Flinch, J.F. (2003) 'Structural evolution of the Sinu-lower Magdalena area (northern Colombia)', in C. Bartolini, R. T. Buffler, and J. Blickwede (ed.) The Circum-Gulf of Mexico and the Caribbean: Hydrocarbon habitats, basin formation, and plate tectonics: AAPG Memoir 79. AAPG, pp. 776–796. https://doi.org/10.1306/M79877C35

[47] Flinch, J. F., & Castillo, V. (2015). Record and constraints of the eastward advance of the Caribbean plate in northern South America. *Petroleum Geology and Potential of the Colombian Caribbean Margin.* Memoir 108. https://doi.org/10.1306/13531930m1082957.

[48] Fulignati, P. (2020). Clay minerals in hydrothermal systems. *Minerals,* 10(10), 919, 17. https://doi.org/10.3390/min10100919.

[49] Galindo, P. (2016). *Transtension and transpression in an oblique subduction setting: Evolution of the Bahia Basin, Colombian Caribbean margin* (Doctoral dissertation, Imperial College London). https://spiral.imperial.ac.uk/bitstream/10044/1/31408/1/Galindo-P-2016-PhD.pdf.

[50] Garzón Varón, F. (2012). Modelamiento estructural de la zona límite entre la microplaca de Panamá y el bloque norandino a partir de la interpretación de imágenes de radar, cartografía geológica, anomalías de campos potenciales y líneas sísmicas. *Departamento de Geociencias.* https://repositorio.unal.edu.co/bitstream/handle/unal/11424/194358.2012.Parte_1.pdf?sequence=7&isAllowed=y.

[51] Gehrels, G. (2011). Detrital zircon U-Pb geochronology: Current methods and new opportunities. *Tectonics of sedimentary basins: Recent advances,* 45-62. https://doi.org/10.1002/9781444347166.ch2.

[52] Geoffroy, L. (2005). Volcanic passive margins. *Comptes Rendus Geoscience,* 337(16), 1395-1408. https://doi.org/10.1016/j.crte.2005.10.006.

[53] Geotec Ltda. (2003) 'Geología de los Cinturones Sinú - San Jacinto. Escala 1: 100 000. *Ingeominas. Memoria Explicativa.* https://recordcenter.sgc.gov.co/B4/13010000020275/documento/pdf/01012027511O1000.pdf.

[54] Ruiz, A. G., Escobar, F. H., Lara, Z. M., Buitrago, N. R., & Lozano, C. L. (2020). Monitoreo sismológico y estudio geoeléctrico somero para evaluar la geodinámica del volcán El Totumo. *INGE CUC,* 16(1). https://doi.org/10.17981/ingecuc.16.1.2020.03.

[55] Gómez, J., Montes, N. E., Alcárcel, F. A., & Ceballos, J. A. (2015). Catálogo de dataciones radiométricas de Colombia en ArcGIS y Google Earth. *Compilando la geología de Colombia: Una visión a 2015,* 63-419. https://www2.sgc.gov.co/MGC/Paginas/pev33ch03.aspx.

[56] Gómez, J., Montes, N. E., Nivia, A., & Diederix, H. (2015). Mapa Geológico de Colombia 2015. Escala 1:1 000 000. *Servicio Geológico Colombiano.* https://www2.sgc.gov.co/MGC/Paginas/mgc_1M2015.aspx

[57] González-Morales, O., Rodríguez-Madrid, A. L., Ríos-Reyes, C. A., & Ojeda-Bueno, G. Y. (2015). Relationship between the mud organic matter content and the maximum height of diapiric domes using analog models. *CT&F-Ciencia, Tecnología y Futuro,* 6(2), 17-32. https://doi.org/10.29047/01225383.17.

[58] Gonzalez-Penagos, F., Milkov, A., Lopez, E., & Duarte, L. (2019, May). Microbial and Thermogenic Petroleum Systems in the Colombian offshore Caribbean—New Geochemical Insights in an Emerging Basin. In 2019 *AAPG Annual Convention and Exhibition:.* https://www.researchgate.net/publication/336591592_Microbial_and_Thermogenic_Petroleum_Systems_in_the_Colombian_offshore_Caribbean_-_New_Geochemical_Insights_in_an_Emerging_Basin

[59] Guzmán, G., Clavijo, J., Barbosa, G., & Salazar, G. (1998). Mapa Geológico de las Planchas 36-37 María La Baja, escala 1: 100,000. *Ingeominas,* p. 1. https://www.semanticscholar.org/paper/Geolog%C3%ADa-de-la-plancha-36-37-Mar%C3%ADa-La-Baja.-Escala-Sgc/678e10e1e2599ffafb5c2dae52ef60604bf459c6

[60] Guzman, G., & Hernandez, R. (1995) 'Geología de la Plancha 38 Carmen de Bolívar'. Bogotá, Colombia: *Ingeominas,* p. 1. https://catalogo.sgc.gov.co/cgi-bin/koha/opac-detail.pl?biblionumber=78466&shelfbrowse_itemnumber=79287.

[61] Guzman, G., Reyes, G. & Ibañez, D. (2003) 'Geología de la Plancha 23 Cartagena'. Bogotá, Colombia: *Ingeominas,* p. 1. https://catalogo.sgc.gov.co/cgi-bin/koha/opac-detail.pl?biblionumber=49581&shelfbrowse_itemnumber=48928.

[62] Hedberg, H. D. (1974). Relation of methane generation to undercompacted shales, shale diapirs, and mud volcanoes. *AAPG Bulletin,* 58(4), 661-673. https://doi.org/10.1306/83d91466-16c7-11d7-8645000102c1865d.

[63] Herrera, C., & Mendoza, C. D. (2018). Evaluación geológica, geotécnica y ambiental de los fenómenos de volcanismo de lodos en la Costa Caribe Colombiana. *Scientia et technica,* 23(1), 104-111. https://doi.org/http://doi.org/10.22517/23447214.16061.

[64] Hillier, S. (1993). Origin, diagenesis, and mineralogy of chlorite minerals in Devonian lacustrine mudrocks, Orcadian Basin, Scotland. *Clays and clay minerals,* 41, 240-259. https://doi.org/10.1346/CCMN.1993.0410211.

[65] Zuluaga, C., Ochoa, A., Muñoz, C., Guerereo, N., Martinez, A. M., Medina, P., ... & Zapata, V. (2009). Proyecto de Investigación: Cartografía e historia geológica de la Alta Guajira. implicaciones en la búsqueda de recursos minerales. *Memoria de las planchas,* 2(3), 5.

[66] Jaboyedoff, M., Bussy, F., Kubler, B., & Thelin, P. (2001). Illite "crystallinity" revisited. *Clays and clay minerals,* 49(2), 156-167.https://doi.org/10.1346/CCMN.2001.0490205.

[67] Jaramillo, C. A., Rueda, M., & Torres, V. (2011). A palynological zonation for the Cenozoic of the Llanos and Llanos Foothills of Colombia. *Palynology,* 35(1), 46-84. https://doi.org/10.1080/01916122.2010.515069.

[68] Jaramillo, J. S., Cardona, A., Monsalve, G., Valencia, V., & León, S. (2019). Petrogenesis of the late Miocene Combia volcanic complex, northwestern Colombian Andes: Tectonic implication of short term and compositionally heterogeneous arc magmatism. *Lithos, 330,* 194-210. https://doi.org/10.1016/j.lithos.2019.02.017.

[69] Jiang, G. J., Angelier, J., Lee, J. C., Chu, H. T., Hu, J. C., & Mu, C. H. (2011). Faulting and Mud Volcano Eruptions Inside of the Coastal Range During the 2003 M w= 6.8 Chengkung Earthquake in Eastern Taiwan. *Terrestrial, Atmospheric & Oceanic Sciences,* 22(5). https://doi.org/10.3319/TAO.2011.04.22.01(TT).

[70] Kassi, A. M., Khan, S. D., Bayraktar, H., & Kasi, A. K. (2014). Newly discovered mud volcanoes in the Coastal Belt of Makran, Pakistan—tectonic implications. *Arabian Journal of Geosciences,* 7, 4899-4909. Available at: https://doi.org/10.1007/s12517-013-1135-7.

[71] Kellogg, J. N., Vega, V., Stallings, T. C., & Aiken, C. L. (1995). Tectonic development of Panama, Costa Rica, and the Colombian Andes: constraints from global positioning system geodetic studies and gravity. *Special Papers-Geological Society of America,* 75-90. https://doi.org/10.1130/SPE295-p75.

[72] Kellogg, J. N., & Bonini, W. E. (1982). Subduction of the Caribbean plate and basement uplifts in the overriding South American plate. *Tectonics,* 1(3), 251-276. https://doi.org/10.1029/TC001i003p00251.

[73] Kennan, L., & Pindell, J. L. (2009). Dextral shear, terrane accretion and basin formation in the Northern Andes: best explained by interaction with a Pacific-derived Caribbean Plate?. *Geological Society, London, Special Publications,* 328(1), 487-531. https://doi.org/10.1144/SP328.20.

[74] Kopf, A. J. (2002). Significance of mud volcanism. Reviews of geophysics, 40(2), 2-1. https://doi.org/10.1029/2000RG000093.

[75] Laguna, O. H., MOLINA, C., Moreno, S., & Molina, R. (2008). Naturaleza mineralógica de esmectitas provenientes de la formación Honda (Noreste del Tolima Colombia). *Boletín de Ciencias de la Tierra,* (23), 55-68. http://www.scielo.org.co/scielo.php?script=sci_arttext&pid=S0120-36302008000200006.

[76] Lara, M., Cardona, A., Monsalve, G., Yarce, J., Montes, C., Valencia, V., ... & López-Martínez, M. (2013). Middle Miocene near trench volcanism in northern Colombia: A record of slab tearing due to the simultaneous subduction of the Caribbean Plate under South and Central America. Journal of South American Earth Sciences, 45, 24-41. https://doi.org/10.1016/j.jsames.2012.12.006.

[77] Laverde, F. (2000). The Caribbean Basin of Colombia, a composite Cenozoic accretionary wedge with under-explored hydrocarbon potential., *VII Simposio Bolivariano - Exploración Petrolera en las Cuencas Subandinas,* pp. 394-410. https://doi.org/10.3997/2214-4609-pdb.118.027eng.

[78] León, S., Cardona, A., Parra, M., Sobel, E. R., Jaramillo, J. S., Glodny, J., ... & Pardo-Trujillo, A. (2018). Transition from collisional to subduction-related regimes: An example from Neogene Panama-Nazca-South America interactions. *Tectonics,* 37(1), 119-139. https://doi.org/10.1002/2017TC004785.

[79] Leslie, S. C., & Mann, P. (2016). Giant submarine landslides on the Colombian margin and tsunami risk in the Caribbean Sea. *Earth and Planetary Science Letters,* 449, 382-394. https://doi.org/10.1016/j.epsl.2016.05.040.

[80] López, E. (2019). Mass balance of sediments in the NW corner of South America. AAPG 2019 *International Conference & Exhibition - Buenos Aires.* https://doi.org/10.13140/RG.2.2.15165.61920.

[81] López-Ramos, E. (2016). Hydrocarbon generation models along the basal detachment of the andean subduction zone in northern ecuador to southern colombia. *CT&F-Ciencia, Tecnología y Futuro, 6*(3), 25-52. https://doi.org/10.29047/01225383.08.

[82] López-Ramos, E., Rincón-Martínez, D., Moreno, N., & Gómez, P. D. (2021). Mass balance of Neogene sediments in the Colombia Basin relationship with the evolution of the Magdalena and Cauca River basins. *CT&F-Ciencia, Tecnología y Futuro,* 11(1), 65-96. https://doi.org/10.29047/01225383.297.

[83] Di Luccio, D., Guerra, I. M. B., Valero, L. E. C., Giraldo, D. F. M., Maggi, S., & Palmisano, M. (2021). Physical and geochemical characteristics of land mud volcanoes along Colombia's Caribbean coast and their societal impacts. *Science of The Total Environment,* 759, 144225. https://doi.org/10.1016/j.scitotenv.2020.144225.

[84] Lutz, R., Littke, R., Gerling, P., & Bönnemann, C. (2004). 2D numerical modelling of hydrocarbon generation in subducted sediments at the active continental margin of Costa Rica. *Marine and Petroleum Geology,* 21(6), 753-766. https://doi.org/10.1016/j.marpetgeo.2004.03.005.

[85] Madonia, P., Grassa, F., Cangemi, M., & Musumeci, C. (2011). Geomorphological and geochemical characterization of the 11 August 2008 mud volcano eruption at S. Barbara village (Sicily, Italy) and its possible relationship with seismic activity. *Natural Hazards and Earth System Sciences,* 11(5), 1545-1557. https://doi.org/10.5194/nhess-11-1545-2011.

[86] Manga, M., Brumm, M., & Rudolph, M. L. (2009). Earthquake triggering of mud volcanoes. *Marine and Petroleum Geology,* 26(9), 1785-1798. https://doi.org/10.1016/j.marpetgeo.2009.01.019.

[87] Mantilla, A.M. (2007). Crustal Structure of the Southwestern Colombian Caribbean. *Dissertation Friedrich-Schiller-Universität Jena, Insitut für Geowissenschaften.* https://www.db-thueringen.de/servlets/MCRFileNodeServlet/dbt_derivate_00014613/Mantilla/Dissertation.pdf

[88] Martinelli, G., & Judd, A. (2004). Mud volcanoes of Italy. *Geological Journal,* 39(1), 49-61. https://doi.org/10.1002/gj.943.

[89] Martinez, J. A., Castillo, J., Ortiz-Karpf, A., Rendon, L., Mosquera, J. C., & Vega, V. (2015). Deep water untested oil-play in the Magdalena Fan, Caribbean Colombian Basin. https://doi.org/10.1306/13531955m1083658.

[90] Martinez, W., Hermoza, W., Espino, D., Carrington, J., Perez, J., Pate, K., & Rodrigo, M. (2015). Tectono-stratigraphic Evolution of the Chichibacoa–Rancherias Basin Offshore Colombia. *Petroleum Geology and Potential of the Colombian Caribbean Margin,* in Memoir 108. https://doi.org/10.1306/13531954m1083657.

[91] Mazzini, A., & Etiope, G. (2017). Mud volcanism: An updated review. *Earth-Science Reviews,* 168, 81-112. https://doi.org/10.1016/j.earscirev.2017.03.001.

[92] McCourt, W. J., Aspden, J. A., & Brook, M. (1984). New geological and geochronological data from the Colombian Andes: continental growth by multiple accretion. *Journal of the Geological Society,* 141(5), 831-845. https://doi.org/10.1144/gsjgs.141.5.0831.

[93] Milkov, A. V., & Etiope, G. (2018). Revised genetic diagrams for natural gases based on a global dataset of> 20,000 samples. *Organic geochemistry,* 125, 109-120. https://doi.org/10.1016/j.orggeochem.2018.09.002.

[94] Milkov, A. V. (2000). Worldwide distribution of submarine mud volcanoes and associated gas hydrates. *Marine Geology,* 167(1-2), 29-42. https://doi.org/10.1016/S0025-3227(00)00022-0.

[95] Milkov, A. V. (2011). Worldwide distribution and significance of secondary microbial methane formed during petroleum biodegradation in conventional reservoirs. *Organic Geochemistry,* 42(2), 184-207.https://doi.org/10.1016/j.orggeochem.2010.12.003.

[96] Milkov, A. V. (2020). Secondary microbial gas. *Hydrocarbons, oils and lipids: Diversity, origin, chemistry and fate*, 613-622. https://doi.org/10.1007/978-3-319-54529-5_22-1.

[97] Mitra, R., Chakrabarti, G., & Shome, D. (2018). Geochemistry of the Palaeo–Mesoproterozoic Tadpatri shales, Cuddapah Basin, India: Implications on provenance, paleoweathering and paleoredox conditions. *Acta Geochimica*, 37, 715-733. https://doi.org/10.1007/s11631-017-0254-3.

[98] Mora, H., Carvajal, J. H., Ferrero, A., León, H., & Andrade, C. A. (2018). Sobre emanaciones de gas natural y la evidencia preliminar de subsidencia en la bahía Cartagena de Indias (Colombia). *Boletín Científico CIOH*, 37, 35–51. https://doi.org/10.26640/22159045.2018.448.

[99] Mora, J. A., Oncken, O., Le Breton, E., Mora, A., Veloza, G., Vélez, V., & de Freitas, M. (2018). Controls on forearc basin formation and evolution: Insights from Oligocene to Recent tectono-stratigraphy of the Lower Magdalena Valley basin of northwest Colombia. *Marine and Petroleum Geology*, 97, 288-310. https://doi.org/10.1016/j.marpetgeo.2018.06.032.

[100] Mora–Bohórquez, J. A., Oncken, O., Le Breton, E., Ibañez–Mejia, M., Veloza, G., Mora, A., ... & De Freitas, M. (2020). Formation and evolution of the Lower Magdalena Valley Basin and San Jacinto fold belt of northwestern Colombia: Insights from Upper Cretaceous to recent tectono–stratigraphy. *The Geology of Colombia*, 3, 21-66. https://doi.org/10.32685/pub.esp.37.2019.02.

[101] Mora-Páez, H., Kellogg, J. N., Freymueller, J. T., Mencin, D., Fernandes, R. M., Diederix, H., ... & Corchuelo-Cuervo, Y. (2019). Crustal deformation in the northern Andes–A new GPS velocity field. *Journal of South American Earth Sciences*, 89, 76-91. https://doi.org/10.1016/j.jsames.2018.11.002.

[102] Naranjo-Vesga, J., Ortiz-Karpf, A., Wood, L., Jobe, Z., Paniagua-Arroyave, J. F., Shumaker, L., ... & Galindo, P. (2020). Regional controls in the distribution and morphometry of deep-water gravitational deposits along a convergent tectonic margin, Southern Caribbean of Colombia. *Marine and Petroleum Geology*, 121, 104639. https://doi.org/10.1016/j.marpetgeo.2020.104639.

[103] NASA, M. (2019). AIST, Japan Spacesystems and US/Japan ASTER Science Team: ASTER Global Digital Elevation Model V003, NASA EOSDIS Land Processes DAAC [data set]. https://doi.org/https://doi.org/10.5067/ASTER/ASTGTM.003.

[104] Oluwadebi, A.G. (2015). The Significance of Crystallinity in Hydrothermal Alteration Mapping: A Case Study of Alem Tena Area of Main Ethiopia Rift , Ethiopia. *International Research Journal of Earth Sciences*, 3(4), 12–17. https://www.semanticscholar.org/paper/The-Significance-of-Crystallinity-in-Hydrothermal-A/973d4073bf8014ad381adfabbfc6f7c2878ae5a4.

[105] Ortiz Karpf, A. L. (2016). *Bathymetric and substrate controls on submarine mass-transport emplacement processes and channel-levee complex evolution* (Doctoral dissertation, University of Leeds). https://etheses.whiterose.ac.uk/15305/1/Ortiz-Karpf-PhD-Thesis-Final.pdf.

[106] Planke, T.A. (2005). Constrains for Th/La on sediment recycling at subduction zones and the evolution of the continents. *Journal of Petrology*, 46(5), 921–944. https://doi.org/10.1093/petrology/egi005.

[107] Quintero Ramírez, J. D. (2012). *Interpretación sísmica de volcanes de lodo en la zona occidental del abanico del delta del río Magdalena, Caribe colombiano* (Bachelor's thesis, Universidad EAFIT). https://repository.eafit.edu.co/bitstream/handle/10784/736/Quintero%20Ram%C3%ADrez_Juan%20David_2012.pdf?sequence=1.

[108] Ramirez, V., Vargas, L. S., Rubio, C., Nino, H., & Mantilla, O. (2015). Petroleum systems of the Guajira Basin, northern Colombia. *AAPG Memoir* 108. AAPG. 141–150. https://doi.org/10.1306/13531944M1083647.

[109] Reed, D. L., Silver, E. A., Tagudin, J. E., Shipley, T. H., & Vrolijk, P. (1990). Relations between mud volcanoes, thrust deformation, slope sedimentation, and gas hydrate, offshore north Panama. *Marine and Petroleum Geology*, 7(1), 44-54. https://doi.org/10.1016/0264-8172(90)90055-L.

[110] Restrepo, I. C., Ojeda, G. Y., & Correa, I. D. (2007). Geomorfología de la plataforma somera del departamento de córdoba, costa caribe colombiana. *Boletín de Ciencias de la Tierra*, (20), 39-52. http://www.scielo.org.co/scielo.php?script=sci_arttext&pid=S0120-36302007000100002.

[111] Restrepo-Pace, P. A., & Cediel, F. (2010). Northern South America basement tectonics and implications for paleocontinental reconstructions of the Americas. *Journal of South American Earth Sciences*, 29(4), 764-771. https://doi.org/https://doi.org/10.1016/j.jsames.2010.06.002.

[112] Reyes, G., Barbosa, G., & Zapata, G. (1998). Geología de la Plancha 29 – 30 Arjona. *Ingeominas*. p (1). https://catalogo.sgc.gov.co/cgi-bin/koha/opac-detail.pl?biblionumber=49584.

[113] Reyes, G., Barrera, R., & Guzman, G. (1998). Geología de la Plancha 31 Campo de la Cruz. *Ingeominas*. p (1). https://catalogo.sgc.gov.co/cgi-bin/koha/opac-detail.pl?biblionumber=49585

[114] Rincón Martínez, D.A. *et al.* (2021) *Geomorfología del fondo marino profundo en la región sur del Caribe Colombiano, Geomorfología del fondo marino profundo en la región sur del Caribe Colombiano.* https://doi.org/10.29047/9789589287361.

[115] Rodríguez, G., & Londoño, A.C. (2002) Mapa Geológico del departamento de la Guajira. Ingeominas. https://doi.org/10.13140/2.1.4852.0008

[116] Rodríguez, I. (2020) *Estructura de la parte sumergida del Cinturón de Sinú y de la parte adyacente de la cuenca de Colombia (margen caribeño al NO de Colombia)*. Tesis Universidad de Oviedo. https://dialnet.unirioja.es/servlet/tesis?codigo=300930

[117] Rossello, E. A., Osorio, J. A., & López-Isaza, S. (2022). El diapirismo argilocinético del Margen Caribeño Colombiano: una revisión de sus condicionantes sedimentarios aplicados a la exploración de hidrocarburos. *Boletín de Geología*, 44(1), 15-48. https://doi.org/10.18273/revbol.v44n1-2022001.

[118] Saha, S., Reza, A. H. M. S., & Roy, M. K. (2020). Illite crystallinity index an indicator of physical weathering of the sediments of the Tista River, Rangpur, Bangladesh. *Int J Adv Geosci*, 8(1), 27-32. https://doi.org/10.14419/ijag.v8i1.30551.

[119] Sanabria, D. S., & Ramirez, V. O. (2018). South Caribbean Petroleum Systems: An Updated Overview. In *AAPG Annual Convention and Exhibition*. https://www.searchanddiscovery.com/documents/2018/11059ramirez/ndx_ramirez.pdf.

[120] Satyana, A. H. (2008). Mud diapirs and mud volcanoes in depressions of Java to Madura: origins, natures, and implications to petroleum system. https://doi.org/10.29118/IPA.947.08.G.139.

[121] Sautkin, A., Talukder, A. R., Comas, M. C., Soto, J. I., & Alekseev, A. (2003). Mud volcanoes in the Alboran Sea: evidence from micropaleontological and geophysical data. *Marine Geology*, 195(1-4), 237-261. https://doi.org/10.1016/S0025-3227(02)00691-6.

[122] Shepard, F. P., Dill, R. F., & Heezen, B. C. (1968). Diapiric intrusions in foreset slope sediments off Magdalena delta, Colombia1. *AAPG Bulletin*, 52(11), 2197-2207. https://doi.org/10.1306/5D25C55F-16C1-11D7-8645000102C1865D

[123] Silva-Arias, A., Páez-Acuña, L. A., Rincón-Martínez, D., Tamara-Guevara, J. A., Gomez-Gutierrez, P. D., López-Ramos, E., ... & Valencia, V. (2016). Basement characteristics in the lower magdalena valley and the sinú and san jacinto fold belts: evidence of a late cretaceous magmatic arc at the south of the colombian caribbean. *CT&F-Ciencia*, Tecnología y Futuro, 6(4), 5-36. https://doi.org/10.29047/01225383.01.

[124] Sohn, I. G. (1961). Techniques for preparation and study of fossil ostracodes. *Moore, RC & Pitrat*, CW, 64-70.

[125] Tabares, N., Soltau, J. M., & Díaz, J. (1996). Caracterización geomorfológica del sector suroccidental del mar Caribe. *Boletín Científico CIOH*, (17), 3-16. https://doi.org/10.26640/22159045.80.

[126] Tobin, H. J., Moore, J. C., Mackay, M. E., Orange, D. L., & Kulm, L. D. (1993). Fluid flow along a strike-slip fault at the toe of the Oregon accretionary prism: Implications for the geometry of frontal accretion. *Geological Society of America Bulletin*, 105(5), 569-582. https://doi.org/10.1130/0016-7606(1993)105<0569:FFAASS>2.3.CO;2.

[127] Toto, E. A., & Kellogg, J. N. (1992). Structure of the Sinu-San Jacinto fold belt—an active accretionary prism in northern Colombia. *Journal of South American Earth Sciences*, 5(2), 211-222. https://doi.org/10.1016/0895-9811(92)90039-2.

[128] Traverse, A. (2007). Paleopalynology. Second edition, *Topics in geobiology*. Springer. https://doi.org/10.1007/978-1-4020-5610-9

[129] Trejos-Tamayo, R., Vallejo, F., Arias, V., García, C., Pardo-Trujillo, A., Bedoya, E., & Flores, J. A. (2020). Biostratigraphy of ejected material from mud volcanoes in the Caribbean region of Colombia: Contribution to the stratigraphy of Sinú Basin. *Journal of South American Earth Sciences*, 103, 102782. https://doi.org/10.1016/j.jsames.2020.102782.

[130] Vargas Jiménez, C. A., & DURÁN TOVAR, J. P. (2005). State of strain and stress in northwestern of South America. *Earth Sciences Research Journal*, 9(1), 41-49. http://www.scielo.org.co/scielo.php?script=sci_arttext&pid=S1794-61902005000100005.

[131] Vermeesch, P., Resentini, A., & Garzanti, E. (2016). An R package for statistical provenance analysis. *Sedimentary Geology*, 336, 14-25. Available at: https://doi.org/10.1016/j.sedgeo.2016.01.009.

[132] Villagómez, D., Spikings, R., Mora, A., Guzmán, G., Ojeda, G., Cortés, E., & Van Der Lelij, R. (2011). Vertical tectonics at a continental crust-oceanic plateau plate boundary zone: Fission track thermochronology of the Sierra Nevada de Santa Marta, Colombia. *Tectonics*, 30(4). https://doi.org/10.1029/2010TC002835.

[133] Villagomez Diaz, D. (2010). *Thermochronology, geochronology and geochemistry of the Western and Central cordilleras and Sierra Nevada de Santa Marta, Colombia: The tectonic evolution of NW South America* (Doctoral dissertation, University of Geneva). https://www.academia.edu/4267944/Thermochronology_geochronology_and_geochemistry_of_the_Western_and_Central_cordilleras_and_Sierra_Nevada_de_Santa_Marta_Colombia_The_tectonic_evolution_of_NW_South_America.

[134] Weber, M. B. I., Cardona, A., Paniagua, F., Cordani, U., Sepúlveda, L., & Wilson, R. (2009). The Cabo de la Vela Mafic-Ultramafic Complex, Northeastern Colombian Caribbean region: A record of multistage evolution of a Late Cretaceous intra-oceanic arc. *Geological Society, London, Special Publications*, 328(1), 549-568. https://doi.org/10.1144/SP328.22.

[135] Wu, D., Pan, J., Xia, F., Huang, G., & Lai, J. (2019). The mineral chemistry of chlorites and its relationship with uranium mineralization from Huangsha uranium mining area in the Middle Nanling Range, SE China. *Minerals*, 9(3), 199. https://doi.org/10.3390/min9030199.

[136] Yamada, H., Nakazawa, H., Yoshioka, K., & Fujita, T. (1991). Smectites in the montmorillonite-beidellite series. *Clay Minerals*, 26(3), 359-369. https://doi.org/10.1180/claymin.1991.026.3.05.

[137] Zuluaga, C., & Stowell, H. (2012). Late Cretaceous–Paleocene metamorphic evolution of the Sierra Nevada de Santa Marta: Implications for Caribbean geodynamic evolution. *Journal of South American Earth Sciences*, 34, 1-9. https://doi.org/10.1016/j.jsames.2011.10.001.

AUTHORS

Eduardo López-Ramos
Affiliation: ECOPETROL S.A
ORCID: https://orcid.org/0000-0001-7836-470X
e-mail: Eduardo.lopezra@ecopetrol.com.co

Felipe González-Penagos
Affiliation: Ministerio de minas y Energía
ORCID: https://orcid.org/0000-0003-1287-1527
e-mail: Fgonzalez@minenergia.gov.co

Daniel Andrés Rincón Martínez
Affiliation: ECOPETROL S.A – ICP
ORCID: https://orcid.org/0000-0002-5684-2130
e-mail: daniel.rincon@ecopetrol.com.co

Nestor Raul Moreno Gómez
Affiliation: ECOPETROL S.A – ICP
ORCID: https://orcid.org/0000-0002-7865-2901
e-mail: nestor.moreno@ecopetrol.com.co

How to cite: López-Ramos , E., González-Penagos, F., Rincón- Martínez, D.A., & Moreno-Gómez, N.R. (2022),Detachment levels of colombian caribbean mud volcanoes. *CT&F - Ciencia, Tecnología y Futuro*, 12(2), 49-78. https://doi.org/10.29047/01225383.401